Bacteriophages target membrane-anchored glycopolymers to promote host cell lysis and progeny release

Authors: Amelia C. McKitterick[1,2,3*], Evan W. Lyerly[1,2], and Thomas G. Bernhardt[1,2*]

Affiliations:
[1]Department of Microbiology
Harvard Medical School
Boston, MA 02115

[2]Howard Hughes Medical Institute

[3]Department of Microbiology
University of Massachusetts Chan Medical School
Worcester, MA 01605

*To whom correspondence should be addressed
Thomas G. Bernhardt
Harvard Medical School
Department of Microbiology
Boston, MA 02115
e-mail: thomas_bernhardt@hms.harvard.edu

or

Amelia C. McKitterick
University of Massachusetts Chan Medical School
Department of Microbiology
Worcester, MA 01605
e-mail: amelia.mckitterick@umassmed.edu

ABSTRACT

Most bacteriophages lyse their host cell to release progeny virions. Double-stranded DNA phages typically promote host lysis using a holin-endolysin system. Holins form pores in the cytoplasmic membrane allowing endolysins access to the peptidoglycan (PG) cell wall, which they degrade to weaken the cell envelope and promote osmotic lysis. Phages that infect Proteobacteria also encode a spanin in their lysis cassette that functions to disrupt the host outer membrane. The spanin-requirement for cell lysis provided the first clue that the proteobacterial outer membrane confers mechanical rigidity to the cell envelope. Corynebacteria and mycobacteria also build an outer membrane, but it is made of mycolic acids instead of lipopolysaccharides. Here, we investigated whether the mycomembrane presents a mechanical barrier to phage-induced lysis of corynebacteria. In addition to annotated holin and endolysin genes, mycobacteriophages and corynephages were found to encode a membrane protein we call LysZ in their lysis cassettes. Deletion of *lysZ* in the corynephage Cog blocked lysis of its host *Corynebacterium glutamicum*. Surprisingly, disruption of the host mycomembrane did not correct this phenotype. Instead, a genetic analysis revealed that blocking synthesis of membrane-anchored glycopolymers called lipomannans/lipoarabinomannans (LM/LAMs) can restore plaque formation when LysZ is inactivated. This genetic system also identified the likely flippase that transports decaprenyl-linked mannose units to the extracellular side of the membrane for polymerization into LM/LAM. Overall, our results indicate that lipoglycans like LM/LAMs play roles in mechanically stabilizing bacterial envelopes and that phages use LysZ-like factors to overcome this barrier to promote lysis.

54 **SIGNIFICANCE**

55 Bacteriophages must break down the cell envelope of their host to induce cell lysis for progeny release.
56 Pathogens like *Mycobacterium tuberculosis* and related corynebacteria build complex cell envelopes that are
57 likely to be especially challenging for phages to disrupt. Here, we identify a novel lysis gene called *lysZ* encoded
58 by many mycobacteriophages and corynephages. Using the model organism *Corynebacterium glutamicum*, we
59 show that LysZ is required to induce host lysis. This requirement is overcome by inactivating genes needed for
60 the synthesis of lipid-anchored glycans called lipomannans/lipoarabinomannans (LM/LAMs). These findings
61 reveal that LM/LAMs are likely to play a mechanical role in stabilizing the cell envelope. LM/LAM biogenesis is
62 therefore an attractive target for drugs that disrupt the integrity of mycobacterial envelopes.

63

INTRODUCTION

To release progeny virions at the end of a replication cycle, most bacteriophages induce lysis of their host cell. This abrupt demise of the host bacterium is promoted by phage proteins that disrupt the stress-bearing capabilities of the cell envelope. Internal osmotic pressure then promotes the explosive rupture of the compromised cell. Double-stranded DNA phages typically use a holin-endolysin system to promote cell lysis[1]. During phage replication, holin proteins accumulate in the cytoplasmic membrane[2]. Depending on the phage, the endolysin either accumulates in the cytoplasm or in an inactive conformation in the membrane. At a genetically programmed time in the replication cycle optimized for progeny dispersal, the holins form pores in the membrane to release the endolysins from the cytoplasm or membrane, allowing them to reach their substrate, the peptidoglycan (PG) cell wall. The released endolysins then degrade the wall to trigger osmotic lysis.

In the case of phages that infect diderm Proteobacteria like *Escherichia coli*, the holin and endolysin alone are not sufficient to promote efficient lysis. A third factor called a spanin is needed to destabilize the outer membrane of these bacteria (**Fig. 1A**). Spanins are often encoded just downstream of the holin and endolysin genes in a phage genomic locus referred to as the lysis cassette[3]. In the model bacteriophage λ, the spanin is formed by two proteins Rz and Rz1, with Rz1 encoded entirely within the Rz gene in a different reading frame. Rz is an inner membrane protein and Rz1 is an outer membrane lipoprotein. When the PG layer is destroyed by the endolysin, the Rz and Rz1 proteins are thought to form a transenvelope complex that connects the inner and outer membrane and fuses them to provide the final disruptive blow to the cell envelope[4,5]. Under conditions where the outer membrane is stabilized, such as in the presence of Mg^{2+}, or in the absence of significant sheer forces, mutant phage lacking a spanin fail to complete lysis[6]. The host cell loses its cell shape as expected when the endolysin degrades the PG layer, but the spheroplast is stabilized by the intact outer membrane, which prevents progeny release. This spanin requirement for phage-induced cell lysis provided the first indication that the outer membrane of Gram-negative bacteria provides mechanical stability to the cell envelope in addition to its well-known role as a permeability barrier that provides these organisms with their high intrinsic resistance to antibiotics[7].

Like the Proteobacteria, bacteria belonging to the order Mycobacteriales such as the pathogen *Mycobacterium tuberculosis* and the related model organism *Corynebacterium glutamicum* (*Cglu*) are diderm. They possess a second membrane that covers a complex, multi-layered cell envelope called the mycolata envelope consisting of a PG layer decorated with another polysaccharide called arabinogalactan (AG)[8] (**Fig. 1B**). However, instead of the phospholipids and lipopolysaccharides that make up the Gram-negative outer membrane, this membrane is made of lipid species called mycolic acids. We were therefore curious whether phages that infect members of the Mycobacteriales encode spanin-like factors to overcome this unique mycomembrane barrier. Indeed, some mycobacteriophages encode an esterase called LysB that cleaves linkages between mycolic acids and the AG layer to disrupt the mycomembrane and promote progeny release[9,10]. In this report, we investigate whether corynephages also use mycomembrane disruptors to induce host lysis.

Genome analysis revealed that instead of *lysB* genes, phages that infect *Cglu* encode a membrane protein of unknown function that we call LysZ in their lysis cassette. LysZ is widespread among not only corynephages but also phages that infect a variety of bacteria within the Actinomycetota phylum to which the Mycobacteriales order belongs. Inactivation of LysZ in a model corynephage called Cog that infects *Cglu* was found to block cell lysis. Surprisingly, disruption of the mycomembrane did not rescue the plaque formation defect of a Δ*lysZ* phage. Rather, a genetic analysis revealed that blocking the synthesis of lipid-linked polysaccharides called lipomannans (LMs) and lipoarabinomannans (LAMs) restored plaque forming ability to phages inactivated for LysZ. Notably, this analysis identified the likely flippase that transports decaprenyl-phosphomannose precursors across the membrane for LM/LAM biogenesis. Additionally, mutants defective for late stages of LM/LAM synthesis were found to have growth and shape defects that are likely to be caused by depletion of the decaprenyl lipid carrier. By analogy with the spanin results, we infer that like the outer membrane of Gram-negative bacteria, LM/LAMs play a role in providing mechanical stability to the cell envelopes of the bacteria that produce them.

RESULTS

Genome analysis identifies lysZ as a potential lysis gene in the Corynebacteriales

To understand how corynephages dismantle the envelope of *Cglu*, the genomes of the corynephages CL31 and Cog were analyzed to identify lysis genes. Like most phages, CL31 and Cog have a modular genome organization in which genes with related functions tend to be encoded in the same regions of the genome. Proximal to the tail genes, CL31 and Cog encode what appears to be a three-gene lysis cassette composed of *lysA*, *hol*, and a gene of unknown function (**Fig. 2A**). The *lysA* gene encodes a predicted N-acetylmuramoyl-L-alanine amidase, an enzymatic activity for PG cell wall degradation, indicating that LysA is likely to be the phage endolysin. The *hol* gene is predicted to encode a holin of the Phage_r1t family, members of which contain two transmembrane (TM) domains separated by a short β-turn[11,12]. The last gene in the lysis cassette encodes a protein of unknown function that contains a predicted disordered N-terminal domain, a TM helix, a long α-helical body, a flexible, proline-rich linker, and a C-terminal helix (**Fig. 2A and B**). Based on the results presented below, we have called this protein LysZ. Sequence similarity searches in NCBI identify LysZ sequences in corynephage phi16 and a putative temperate phage in *Cglu* ATCC 13870. Using proximity to endolysin-encoding genes and the predicted structural features of LysZ, we identified *lysZ*-like genes in diverse phages that infect a range of bacteria in the Actinomycetota phylum (**Fig. 2A and B**). These phages include those that infect members if the Mycobacteriales order such as *Mycobacterium smegmatis* and *Gordonia terriae*, as well as bacteria in other related orders such as the Micrococcales. In many of these phages, the *lysZ*-like gene is encoded downstream of a gene predicted to encode a protein with four TM domains (**Fig. 2A**). We have named these proteins LysY due to their location in the putative lysis cassettes of many phages. In this report, we focused on determining the function of the LysZ proteins.

138 ***Cog and CL31 phages require LysZ for normal plaque formation***

139 To determine if *lysZ* is required for host lysis, mutant CL31 and Cog phage deleted for *lysZ* were constructed
140 using CRISPR-Cas engineering. CL31 Δ*lysZ* phage formed smaller plaques than wild-type CL31 on a lawn of
141 the wild-type *Cglu* strain MB001 whereas a Cog mutant lacking *lysZ* had a severe plating defect (**Fig. 2C, S1A-**
142 **B**). The plating defect of Δ*lysZ* Cog phage was complemented by the expression of the cognate *lysZ* gene from
143 a plasmid. Additionally, ^{Cog}*lysZ* complemented the small plaque phenotype of the CL31 Δ*lysZ* phage. A construct
144 expressing ^{CL31}*lysZ* failed to restore the plaquing ability of CL31 Δ*lysZ* or Cog Δ*lysZ* for unknown reasons.
145 However, *lysZ* alleles from the distantly related phages Corndog, Fury, and Smarties that infect *M. smegmatis*
146 *G. terrae*, and *Mirobacterium paraoxydans*, respectively were able to complement the plating defects of the *lysZ*
147 deletion mutants of Cog and CL31 (**Fig. 2C, S1A-B)** The mutant phenotypes and complementation results
148 indicate that LysZ plays an important and likely conserved role in the propagation of phages that infect members
149 of the Mycobacteriales and their relatives.

150

151 ***LysZ is required for host cell lysis but does not target the mycomembrane***

152 In addition to their defects in plaque formation, Cog and CL31 phages deleted for *lysZ* displayed a defect in
153 inducing cell lysis in a liquid infection assay (**Fig. 3A, Fig. S2**). As with the plaquing phenotypes, the lysis defect
154 in liquid medium was complemented by inducing the expression of *lysZ* alleles from a plasmid at the time of
155 infection. These lysis defects were associated with a decrease in phages released during infection (**Fig. 3B**). To
156 further investigate the defect caused by *lysZ* inactivation, we used time-lapse microscopy to follow the changes
157 in cell morphology and cell lysis induced by wild-type Cog or the Δ*lysZ* mutant following the infection of cells with
158 a high multiplicity of infection (MOI). Cells began lysis at about 90 minutes post infection with wild-type Cog, with
159 the majority of cells being lysed after 120 minutes (**Fig. 3C, Movie 1**). By contrast, lysis was not observed up to
160 five hours after infection with the Cog Δ*lysZ* phage. Instead, the cells were observed to progressively become
161 more bulbous and inflated at the poles (**Fig. 3C, Movies 2 and 3**), suggesting that the cell envelope was being
162 partially deconstructed by the phage to cause the loss in cell shape, but that the final step of osmotic lysis was
163 blocked. This result is reminiscent of the observation of stable spheroplasts of *E. coli* formed following infection
164 with phage λ inactivated for its spanin[6]. To determine if the mycomembrane is stabilizing the envelope of *Cglu*
165 cells infected with the Cog Δ*lysZ* phage, we tested whether the loss of LysZ function could be complemented by
166 production of a mycobacteriophage LysB esterase that cleaves mycolic acid-AG linkages[10]. Surprisingly, LysB
167 production did not restore the ability of the Cog Δ*lysZ* phage to form plaques (**Fig. 3D**). Unlike mycobacteria,
168 mutants of *Cglu* lacking the mycomembrane are viable[13]. We therefore also tested whether the Cog Δ*lysZ* phage
169 could form plaques on lawns of *Cglu* mutants inactivated for the *afhA* or *ostA* genes needed for mycolic acid
170 biogenesis[14]. Again, to our surprise, preventing mycomembrane assembly did not rescue the plaque formation
171 defect of the Cog Δ*lysZ* phage (**Fig. 3E**). A similar test for CL31 Δ*lysZ* phage could not be performed because
172 our prior results indicate that CL31 requires the mycomembrane for infection whereas Cog does not[14]. Based on
173 these results, we conclude that LysZ is required by corynephages to promote efficient host cell lysis and that its
174 function is unrelated to mycomembrane disruption.

175

176 ***Mutants defective for decaprenyl-phosphomannose synthesis rescue the Cog Δ*lysZ* plating defect***

177 To identify the layer of the cell envelope targeted by LysZ, we took advantage of the finding that overexpression
178 of ^{Cog}*lysZ* is toxic (**Fig. 4A-C**). Reasoning that spontaneous suppressors resistant to ^{Cog}LysZ production might
179 identify mutants that alter or eliminate the envelope layer that LysZ is required to disrupt, we isolated survivors
180 following the induction of ^{Cog}*lysZ* expression from a plasmid. Among the survivors of ^{Cog}*lysZ* expression, we
181 anticipated a high frequency of isolates harboring plasmids defective for ^{Cog}*lysZ* expression in addition to the
182 mutants of interest. The survivors were therefore screened using two additional assays. The first screen was for
183 isolates hypersensitive to the detergent sodium dodecyl sulfate (SDS). Here, we expected isolates with defective
184 plasmids to retain normal SDS-resistance. However, we expected that mutants with an altered cell envelope
185 conferring LysZ resistance might also have a compromised permeability barrier rendering them sensitive to SDS.
186 We therefore patched survivors of ^{Cog}*lysZ* expression on media with or without SDS and selected those that
187 displayed SDS hypersensitivity. These isolates were then tested for their ability to serve as permissive hosts for
188 the Cog Δ*lysZ* phage. Finally, to map the mutations responsible for the desired phenotypes, mutant isolates that
189 allowed plaque formation by the Cog Δ*lysZ* phage were analyzed by whole genome sequencing.

190

191 Three mutant isolates were identified through this screen (**Fig. 4D-E**). One of the suppressor mutations that
192 promoted LysZ resistance and restored plaque forming ability to the Cog Δ*lysZ* phage was an insertion element
193 that interrupted the *cgp_0855* gene (**Table S1**). This gene is upstream of *manA*, which encodes an enzyme that
194 interconverts fructose-6-phosphate into mannose-6-phosphate for ultimate use in the synthesis of glycolipids like
195 phosphatidylinositol mannosides (PIMs) and LM/LAM glycopolymers in the cell envelope[15] (**Fig. 5A**). The second
196 suppressor harbored three mutations, with one being a single nucleotide change in *manB* (also referred to as
197 *pmmA*), which encodes the enzyme acting after ManA in the synthesis pathway for generating GDP-mannose
198 for use in envelope biogenesis[16] (**Fig. 5A**). Finally, the third suppressor had a mutation mapping to *ppmC*, which
199 encodes the enzyme that uses GDP-mannose created by ManC as a substrate to generate the lipid-linked sugar
200 decaprenyl-phosphomannose (DPM)[17–19] (**Fig. 5A**). Thus, all the isolates from the selection and screening
201 combination had mutations predicted to disrupt DPM biogenesis.

202

203 ***Evidence that LysZ is required to overcome an LM/LAM barrier for Cog to elicit lysis***

204 To validate the results from the suppressor selection/screen, we generated *Cglu* deletion mutants inactivated for
205 ManA, ManB, ManC, and PpmC. As expected, each isogenic deletion mutant conferred resistance to ^{Cog}*lysZ*
206 expression and rescued the plating defect of the Cog Δ*lysZ* phage (**Fig. 5B, 5C, and S3C**). Inactivation of
207 *cgp_0855* did not allow plaque formation by the Cog Δ*lysZ* phage, suggesting that the phenotype of the original
208 *cgp_0855* mutant isolate resulted from a polar effect of the insertion element on the expression of the neighboring
209 *manA* gene (**Fig. S3A**).

210

211 To identify the DPM-related envelope component responsible for inhibiting plaque formation by the Cog Δ*lysZ*
212 phage, we constructed several mutants defective in the conversion of DPM to surface glycans. Following its
213 synthesis, the phosphomannose headgroup of DMP must be externalized by a yet to be identified lipid flippase
214 for its polymerization into mannose-based glycans used for envelope biogenesis. Once flipped, DPM is used to
215 polymerize LM/LAMs on the lipid anchor called acylated phosphatidylinositol mannoside (AcPIM2) or to form a
216 lipomannan variant called LM-B that is linked to the anchor mannosyl-glucuronic acid diacylglycerol (Gl-X)[20]. In
217 both cases, the glycosyltransferase MptB initiates mannan polymerization and the glycosyltransferases MptA
218 and MptC extend the glycan and introduce branches, respectively[21–23] (**Fig. 5A**). Deletion of *mptB* robustly
219 restored plaque formation by Cog Δ*lysZ* (**Fig. 5B**). Complementation of the *mptB*, *manC*, and *ppmC* deletions
220 by expressing the corresponding gene from an ectopic locus restored the observed Cog Δ*lysZ* plaque formation
221 defect (**Fig. S3B**). Inactivation of MptA had an intermediate effect on Cog Δ*lysZ* plaque formation, while loss of
222 MptC had little or no effect on Cog Δ*lysZ* plaque formation, respectively (**Fig. 5B**). Another use of DPM in the
223 envelope is protein mannosylation by the mannosyltransferase Pmt[24] (**Fig. 5A**). Deletion of *pmt* had no effect on
224 the plaquing ability of Cog Δ*lysZ* phage (**Fig. 5B**). Notably, unlike deletion of *ppm*C or other genes required for
225 DPM formation that both restored Cog Δ*lysZ* plaque formation and conferred resistance to LysZ toxicity,
226 inactivation of MptB only affected Cog Δ*lysZ* plaque formation. Cells lacking MptB remained sensitive to ^{Cog}*lysZ*
227 expression (**Fig. 5C**). We therefore conclude that the function of LysZ is to overcome what we infer to be an
228 envelope stabilizing activity of LM/LAMs with the initial phases of mannan polymerization being sufficient to
229 prevent lysis in the absence of LysZ. By contrast, the toxic activity of LysZ only required the presence of DPM,
230 not its downstream products, suggesting that the lysis promoting activity of LysZ may be triggered by its
231 association with the lipid-linked mannose precursor.
232
233 ***MptB inactivation likely results in depletion of the decaprenyl lipid carrier***
234 Loss of LM/LAM production via deletion of *mptA* in *M. smegmatis* was recently shown to cause a growth and cell
235 shape defect when cells are cultured on LB agar but not standard 7H10 medium[25]. This growth defect could be
236 suppressed by increasing the osmolarity of the LB medium with the addition of sorbitol, indicating that the load-
237 bearing, turgor-resistance function of the cell envelope is compromised upon MptA inactivation. We similarly
238 observed that *Cglu* cells lacking MptB, the enzyme upstream of MptA for LM/LAM biogenesis, had shape defects
239 and a severe growth defect on LB medium that is suppressed by sorbitol addition (**Fig. 5D**). Notably, deletion of
240 *ppmC*, which blocks DPM formation, suppressed the growth and shape defects caused by the inactivation of
241 MptB. Based on these results, we conclude that the severity of the Δ*mtpB* phenotype in *Cglu* is likely mediated
242 by the sequestration of the decaprenyl lipid carrier in the DPM pool, causing a reduction in the lipid-carrier
243 dependent process of peptidoglycan synthesis that affects cell growth and shape (see Discussion).
244
245 ***Identification of the likely DPM flippase for LM/LAM biogenesis***
246 Cgp_1254 is a predicted to be a member of the GtrA-like lipid flippase family which has been implicated in
247 transporting polyprenyl-linked sugars across the cytoplasmic membrane[26]. Additionally, inactivation of *cgp_1254*

248 results in a phenotypic fingerprint that is similar to that caused by *ppmC* defects[27]. Thus, Cgp_1254, which we
249 have renamed *dpmF* is an excellent candidate for the as yet unidentified DPM flippase needed for LM/LAM
250 biogenesis. To test this possibility, we took advantage of the Cog Δ*lysZ* mutant as a probe for the production of
251 LM/LAM. Similar to other mutations that negatively impact LM/LAM synthesis, deletion of *dpmF* suppressed the
252 plating defect of the Cog Δ*lysZ* phage (**Fig. 6A**). Moreover, DpmF inactivation resulted a loss of detectable
253 LM/LAM in cell lysates that was comparable to that observed in Δ*mptB* cells with the exception that a small
254 amount of low molecular weight glycans were observed in the Δ*dpmF* mutant (**Fig. 6B**). Accordingly, cells deleted
255 for *dpmF* displayed an intermediate sensitivity to ^{Cog}LysZ overproduction (**Fig. S4**). Cells lacking DpmF were
256 resistant to low levels of ^{Cog}*lysZ* induction, but unlike the Δ*ppmC* mutant, they were sensitive to higher levels of
257 ^{Cog}*lysZ* expression. We therefore conclude that DpmF is likely to be the dedicated flippase that transports DPM
258 across the cytoplasmic membrane for LM/LAM biogenesis. Furthermore, in the absence of DpmF it appears that
259 a low level of DPM transport is mediated by an alternative flippase, enabling the production of a small amount of
260 short LM glycans and rendering cells sensitive to high levels of ^{Cog}LysZ.
261
262
263 **DISCUSSION**
264 Phages that infect bacteria within the Mycobacteriales order require specialized lytic functions to rupture the
265 complex cell envelope of their hosts for the release of progeny virions. Mycobacteriophages supplement the core
266 holin-endolysin system that destroys the peptidoglycan cell wall with LysB esterases that disrupt the
267 mycomembrane by cleaving linkages connecting mycolic acids to the arabinogalactan layer[9,10]. The LysB
268 requirement for efficient host cell lysis indicates that the mycomembrane of mycobacteria serves as a significant
269 barrier to phage progeny dispersal. We were therefore surprised to find that corynephages lack identifiable *lysB*-
270 like genes despite having hosts that also build a mycomembrane. This *lysB* deficiency prompted us to search
271 for other corynephage genes that might encode functions targeting the mycomembrane to induce cell lysis. The
272 *lysZ* gene emerged as a good candidate due to its broad distribution within the lysis cassettes of corynephages
273 and other phages that infect members of the Mycobacteriales order. Indeed, deletion of *lysZ* resulted in a plaque
274 formation and lysis defect for two corynephages Cog and CL31 that infect our model host *Cglu*. Notably, this
275 defect was corrected by plasmid-based expression of *lysZ*-like genes from diverse phages that infect a range of
276 different hosts, indicating that these genes encode a conserved activity required for efficient host cell lysis.
277
278 Genetic analysis of LysZ activity indicated that it is not required to disrupt the mycomembrane as we initially
279 suspected. This result coupled with the lack of *lysB*-like genes in the lysis cassettes of corynephages suggests
280 that the mycomembrane of corynebacteria may not be as formidable a barrier to phage release as the
281 corresponding membrane of mycobacteria, which contains much longer mycolates that are covalently linked to
282 the arabinogalactan layer to a greater degree than in the corynebacterial membrane[28,29]. Rather than targeting
283 the mycomembrane, our results indicate that LysZ proteins are required to overcome a barrier created by
284 LM/LAM lipoglycans. Cells of *Cglu* were rapidly lysed by wildtype phages. However, Cog phage lacking LysZ

285 was not capable of efficiently lysing cells with LM/LAMs, which instead of lysing were converted to misshapen
286 yet osmotically stable protoplast-like cells by the mutant phage. This phenotype is reminiscent of the lysis defect
287 caused by spanin inactivation in phages that infect Gram-negative bacteria[6]. Infections with such phages yield
288 spheroplasts stabilized by the outer membrane, a result that hinted at a stress-bearing role for the outer
289 membrane layer of the envelope that has since been well established[7]. By analogy with the spanins, our results
290 with LysZ and the wide distribution of *lysZ*-like genes among corynephages and mycobacteriophages suggest
291 that LM/LAMs play a similar mechanical role in stabilizing the envelope of *Cglu* and other members of the
292 Mycobacteriales order (**Fig. 7**).
293
294 A recent study of LM/LAM lipoglycans in *M. smegmatis* found that cells lacking the MptA enzyme that elongates
295 LM/LAM polymers display morphological and growth defects, suggesting a role for these molecules in cell shape
296 and division[25]. Blocking a similarly late stage in LM/LAM synthesis in *Cglu* by inactivating the MptB enzyme also
297 results in cell shape and division defects. However, we found that inactivating the enzyme that forms the lipid-
298 linked LM/LAM precursor DPM suppressed this phenotype. This result indicates that the shape and division
299 problems of Δ*mptB* mutants are not caused by the loss of LM/LAM per se but instead are the result of secondary
300 effects stemming from the failure to complete LM/LAM synthesis. This phenomenon is commonly observed in
301 bacterial mutants defective for the synthesis of a surface glycan. For example, defects in the later steps of
302 teichoic acid synthesis in Firmicutes or in enterobacterial common antigen synthesis in *E. coli* cause growth and
303 shape defects that are suppressed by inactivating the enzyme that forms the first lipid-linked intermediate in the
304 respective pathway[30–32]. The problems caused by late-stage blocks in these pathways are thought to arise due
305 to the shared use of the polyprenyl lipid carrier by surface glycan synthesis pathways and the pathway for
306 peptidoglycan cell wall biogenesis. When a glycan synthesis pathway is blocked after the committed step, lipid
307 carrier-linked intermediates of the pathway accumulate, reducing the availability of the carrier. The limited carrier
308 supply then indirectly inhibits/reduces peptidoglycan synthesis to cause the observed growth and morphological
309 defects. Our results with the Δ*mptB* mutants of *Cglu* suggest that the growth and shape defects induced by
310 blocking the late stages of LM/LAM synthesis also stem from indirect effects on peptidoglycan synthesis. We
311 suspect that the indirect inhibition of peptidoglycan synthesis also contributes to the phenotypes observed for
312 MptA inactivation in *M. smegmatis*, but further experiments are required to test this hypothesis.
313
314 Blocking the early stages of LM/LAM synthesis by deleting *ppmC* in *Cglu* results in a growth defect. Although
315 indirect effects are difficult to rule out, this result suggests an important role for LM/LAM polymers for cell growth
316 that is independent of the potential problems with peptidoglycan synthesis induced by late-stage blocks in the
317 LM/LAM synthesis pathway. Why LM/LAM polymers are important for growth is not clear, but the observation
318 that they present a barrier to phage induced lysis suggests that their function may involve the mechanical
319 stabilization of the cell envelope. How these polymers might stabilize the envelope remains unclear, but we
320 envision that networks of hydrogen bonds between adjacent polymers could form a stress-bearing shell around
321 the membrane. Thus, LM/LAM interactions may function analogously to the lateral packing of LPS molecules in

322 the outer membrane of Gram-negative bacteria, the stress-bearing properties of which are dramatically
323 enhanced by the long glycan chains of the O-antigen[7,33]. Bridging interactions between lipid anchored polymers
324 related to LM/LAMs like lipoteichoic acids may also provide structural properties to the envelope of Gram-positive
325 Firmicutes that phages of these bacteria must also disrupt to promote efficient lysis.
326
327 How LysZ overcomes the barrier to lysis presented by the LM/LAM lipoglycans remains unknown. One possibility
328 is that the long helical structure predicted for LysZ interferes with the lateral interactions between LM/LAM
329 polymers that are normally involved in stabilizing the membrane against osmotic rupture. Notably, the toxicity of
330 LysZ overproduction requires DPM production. Thus, another attractive possibility is that LysZ functions similarly
331 to the lantibiotic nisin, which forms pores in the membrane after it binds the lipid-linked PG precursor lipid II[34].
332 Accordingly, LysZ may similarly form a membrane disrupting pore structure following its association with DPM.
333 Further studies of LysZ function and of phage lysis systems in general promises to reveal new insights into the
334 biology of bacterial cell envelopes and how they can be disrupted for potential biotechnological and therapeutic
335 applications.
336
337 **ACKNOWLEDGEMENTS**
338 The authors would like to acknowledge all the members of the Bernhardt and Rudner labs for thoughtful
339 discussion and generous advice. Particularly, we would like to thank Anastacia Parks for creating and sharing
340 the *pmt* and *manA* mutants and Eric Snow for sharing and trouble-shooting LM/LAM analysis protocols. We
341 would like to thank Dr. Graham Hatfull and the SEA-PHAGES program for sharing stocks of the phages Fury
342 and Corndog. We also would like to thank Paula Montero Llopis and her team at the Microscopy Resources on
343 the North Quad (MicRoN) core facility at HMS for the microscopy services. This work was supported by
344 Investigator funds from the Howard Hughes Medical Institute, and ACM was supported in part by the Life
345 Sciences Research Foundation where she was a Simons Fellow.
346
347 **AUTHOR CONTRIBUTIONS**
348 A.C.M. and T.G.B. designed research; A.C.M. and E.W.L. performed research; A.C.M. and T.G.B. analyzed data;
349 A.C.M. and T.G.B. wrote the paper.
350
351
352 **METHODS**
353 **Media, strains, plasmids, and phages**
354 *Cglu* was grown in LB supplemented with 0.4% glucose (LBG) or Brain Heart Infusion supplemented with 9.1%
355 sorbitol (BHIS) at 30°C with aeration. Kanamycin (kan), chloramphenicol (chlor) and apramycin (apra) were
356 added to the media as needed at concentrations of 15 µg/mL, 3 ug/mL and 12.5 µg/mL respectively. Theophylline
357 was used at a concentration of 1 mM and IPTG was used at a concentration of 0.1 mM for induction of gene
358 expression unless otherwise indicated. *E. coli* was grown in LB at 37°C or 30°C with aeration with 25 µg/mL kan

359 or 50 µg/mL apra as needed. All strains, phages plasmids, and primers used are listed in Supplemental Tables
360 S2-S5.
361
362 **Preparation of *Cglu* competent cells and electroporation**
363 Saturated cultures of *Cglu* strains were diluted 1:100 into BHI+supplements (9.1% sorbitol and 2.5% glycine)
364 and grown for 16 hours at 18ºC. Cells were harvested by centrifugation at 3000xg for 10 minutes at 4ºC. The
365 cell pellet was then washed 3 times with cold 10% glycerol and resuspended in 10% glycerol to an approximate
366 OD_{600} of 20. DNA was added to 100 µL aliquots of the electrocompetent cells on ice before being electroporated
367 at 1.7 kV. Once electroporated, cells were immediately flushed with fresh BHIS and heat-shocked for 6 minutes
368 at 46ºC. Cells were then outgrown at 30ºC for 1 hour and plated on antibiotic-containing plates.
369
370 **Plasmid and recombinant DNA construction**
371 Details on plasmid assembly can be found in Supplementary Methods. Assembled *Cglu* plasmids were
372 transformed into *E. coli* or electroporated directly into *Cglu*. Linear *Cglu* recombination cassettes were generated
373 with 50 to 500 base pairs of homology upstream and downstream of the desired deletion. These cassettes were
374 assembled either by direct amplification of a kanamycin cassette from plasmid pSEC01 or pEWL74 using primers
375 with 50bp of homology to the chromosome and 20bp to the cassette or through amplification of the homologous
376 regions and assembly with the kanamycin cassette using overlapping extension (SOE) PCR.
377
378 To establish a stable ^{Cog}*lysZ* expression plasmid, a pTGR5[35] derivative was created with a theophylline-inducible
379 translational *riboE1* riboswitch[36] replacing the ribosome biding site of pTGR5 to make pACM40. ^{Cog}*lysZ* was
380 cloned into this vector via isothermal assembly (ITA) and transformed into E. coli. Upon transformation into *Cglu*,
381 individual colonies were picked and patched in the presence and absence of inducer to confirm the maintenance
382 of ^{Cog}*lysZ* toxicity. Plasmid from an isolate displaying a high degree of inducer sensitivity was then sequenced
383 and found to have an A>G point mutation between the P_{tac} and *riboE1* (pACM387). This plasmid, with expression
384 control referred to as P_{tac}*riboE1 was then further used for expression studies throughout this work.
385
386 **Strain construction**
387 *Allelic exchange*
388 Clean deletions were generated through the use of the pCRD206 temperature sensitive plasmid[37], wherein 500-
389 1kb fragments were amplified upstream and downstream of the desired gene. These fragments were assembled
390 into pCRD206 via ITA. Plasmids were then electroporated into *Cglu* and grown at 25ºC. Successful transformants
391 were then purified at 30ºC to select for integration. Integrants were then outgrown at 25ºC and plated on 10%
392 sucrose at 30ºC to select for double-crossover events. The presence of the desired deletion allele was then
393 validated through diagnostic PCR.
394
395 *Recombineering*

396 *Cglu* strains were engineered through recombineering as described by Hart et al.[38] using a single-stranded
397 annealing protein (SSAP) and cognate single-stranded binding protein (SSB) from a from *Troponema socranskii*
398 prophage[39]. Briefly, the recombineering plasmid (pEWL54 or pEWL103) was electroporated into MB001. For
399 pEWL54, cells were grown at 30ºC in BHIS chlor. An overnight culture of the pEWL54 recombineering strain was
400 then back diluted 1:50 into BHI+supplements (9.1% sorbitol and 2.5% glycine) and grown at 30ºC with aeration.
401 After ~3 hours when the cells were mid-log, the SSAP/SSB pair were induced with 1mM PTG and grow was
402 continued with aeration for 2 more hours. These cells were then harvested as described above. A total of 1µg of
403 DNA was added to each 100 µL aliquot of electrocompetent cells and electroporated as above. Cells were plated
404 on BHIS kan and grown at 30ºC. Colony PCR was used to determine successful recombination events, and
405 colonies were patched in the presence and absence of chlor to monitor loss of the recombineering plasmid.
406
407 For pEWL103, which is temperature-sensitive for replication, cells were grown at 25ºC in BHIS apra. An overnight
408 culture of the pEWL103 strain was then back diluted 1:50 and grown at 25ºC with aeration in BHI+supplements.
409 After ~4 hours when the cells were mid-logarithmic phase, the SSAP/SSB pair was then induced with 1mM
410 theophylline and 1 mM IPTG and growth was continued with aeration for 4 more hours. These cells were then
411 harvested as described above and 1 µg DNA template was added to each 100 µL aliquot of electrocompetent
412 cells. Cells were electroporated as above and outgrown for 2 hours at 25ºC. Cells were then plated on BHIS kan
413 at 25ºC. Colony PCR was used to determine successful recombination events, and colonies were then grown at
414 30ºC to cure the recombineering plasmid. To make an unmarked deletion, strains were recombineered with a
415 kanR cassette flanked by *loxP* sites as above. Once confirmed, such mutants were electroporated with pCre and
416 grown for two days at 25ºC. Colonies were then purified and grown at 30ºC overnight to cure the plasmid.
417 Individual colonies were then picked and patched onto media with and without kan or apra to identify
418 transformants that lost both the resistance cassette and the pCre plasmid. Colony PCR was used to determine
419 successful recombination events.
420
421 **Bacterial viability assays**
422 The optical density of overnight bacterial cultures was normalized to OD_{600}=1 and serially diluted 10-fold. A
423 volume of 5 µl of each dilution was spotted onto a plate and allowed to dry. Plates were incubated at 30ºC for
424 one or two nights before imaging.
425
426 **Bacterial growth kinetics**
427 Overnight cultures of *Cglu* were diluted 1:100 into LBG apra and grown to midlog. Cultures were normalized to
428 an OD_{600}=0.15 and added to a 96-well plate with 0.1 mM IPTG and 1 mM theophylline in biological triplicates
429 and technical duplicates. Optical density was measured every 10 minutes with shaking at 30ºC over the course
430 of 16 hours in a Tecan Nano.
431
432 **Bacterial colony forming unit (CFU) measurement**

433 Overnight cultures of *Cglu* were diluted 1:100 into LBG apra and grown to midlog. Cultures were normalized to
434 an OD_{600}=0.4 and serially tenfold diluted. A volume of 100 µL of each dilution was plated for single colonies in
435 technical duplicates and incubated overnight at 30°C. The normalized cultures were induced with 0.1 mM IPTG
436 and 1 mM theophylline overnight. In the morning, the OD_{600} for each culture was recorded and serially diluted. A
437 volume of 100 µL of each dilution was plated for single colonies in technical duplicates and incubated overnight
438 at 30°C. Fold chance in CFU was calculated by dividing the CFU post-induction by the CFU pre-induction.
439 Experiments were performed in biological triplicates.
440

441 **Phage propagation and genetic manipulation**

442 ***Cglu* phages**

443 For isolation and enumeration of phage stocks, *Cglu* hosts were grown to mid-log (OD_{600} = 0.3-0.5) in LBG
444 supplemented with 10mM $CaCl_2$ and 100 µL cells were mixed with 10 µL of phage diluted in SM buffer and
445 allowed to adsorb for 10 minutes. The mixture was then added to LBG 0.5% agar supplemented with 10 mM
446 $CaCl_2$, spread on normal agar, and allowed to solidify. Solid plates were incubated overnight at 30°C. Confluent
447 lysis plates were used to grow high titer phage stocks. These plates were overlayed with SM buffer and gently
448 rocked overnight at 4°C. Overlays were then harvested and filter sterilized before being concentrated in a
449 centrifugal column (Amicon 100 kDa).
450

451 Mutations in *lysZ* were achieved through modification of a Cas12 system[40] (see Plasmid Construction). First, WT
452 phage was plated onto midlog *Cglu* grown in LBG 10mM $CaCl_2$ containing a multi-copy plasmid encoding the
453 desired mutations with ~200bp of homology on either side. Ten plaques from this host were picked and pooled.
454 Next, successfully recombined phages were selected on *Cglu* containing a CRISPR-Cas12 system with a spacer
455 against the *lysZ* allele of interest. For this step, the cells were grown in LBG 10 mM $CaCl_2$ with 3 µg/mL chlor
456 and the CRISPR-Cas12 system was induced with 1 mM IPTG and 1 mM theophylline. To enable selection of
457 Cog Δ*lysZ* phages, the CRISPR-Cas plasmid pACM351 was electroporated into *Cglu* Δ*cgp_1254* and used as
458 a Δ*lysZ* permissive host. Individual plaques were picked and validated by colony PCR and Sanger sequencing.
459 Desired plaques were then repurified 2x on the CRISPR host and stored in SM buffer.
460

461 **Phage plaque formation assays**

462 Phage spot assays with hosts encoding toxic lysis genes were performed by concentrating 2 mL of a *Cglu*
463 overnight with apra into 500 µL. Then, 200 µL concentrated *Cglu* culture was added to 4 mL molten top LBG
464 0.5% agar supplemented with 10 mM $CaCl_2$, 12.5 µg/mL apra, 0.1 mM IPTG and with or without 1 mM
465 theophylline as indicated in the figure legends, vortexed, applied over a solid LBG 1.5% agar plate, and allowed
466 to dry under a flame for 10 minutes. Phage spot assays for mannose mutants were performed by concentrating
467 4 mL of a mid-log *Cglu* culture into 500 µL. Then, 200 µL concentrated *Cglu* culture was added to 4 mL molten
468 top LBG 0.5% agar supplemented with 10 mM $CaCl_2$, vortexed, applied over a solid LBG 1.5% agar plate, and
469 allowed to dry under a flame for 10 minutes. Phage spot assays for complementation of mannose mutants were

470 performed by subculturing an overnight culture into fresh media with apra, 1mM theophylline, and 0.01 mM or
471 0.1 mM IPTG as indicated in the figure legend, growing to mid-log. Then, 4 mL of these cultures were
472 concentrated into 500 µL and 200 µL *Cglu* culture was added to 4 mL molten top LBG 0.5% agar supplemented
473 with 10 mM $CaCl_2$, apra, 1 mM theophylline, and 0.01 mM or 0.1 mM IPTG, vortexed, applied over a solid LBG
474 1.5% agar plate, and allowed to dry under a flame for 10 minutes. Phage were diluted tenfold, and spots of 3 µL
475 of each dilution were applied to the solidified top agar and allowed to dry under flame. Dried plates were then
476 incubated overnight at 30 C. Phage plaque assays were performed by subculturing overnight cultures into fresh
477 LBG with apra and 10 mM $CaCl_2$ and outgrown to midlog. Then, 100 µL of cells and 10 µL of phage dilutions
478 were mixed and allowed 10 minutes to adsorb. This mixture was then plated with LBG 0.25% or 0.5% top agar
479 as labeled with 10 mM $CaCl_2$, apra, 1 mM theophylline, and 0.1 mM IPTG. The plates were then allowed to
480 solidify before being incubated overnight at 30°C.
481
482 **Phage lysis kinetics**
483 Overnight *Cglu* cultures were subcultured 1:100 into LBG supplemented with 10 mM $CaCl_2$ and apra and grown
484 to midlog. Cultures were normalized to an OD_{600}=0.25 and added into a 96 well plate. Phage was added at an
485 MOI of 2.5 and cells were induced upon infection with addition of 0.1 mM IPTG and 1 mM theophylline. The plate
486 was incubated in the Tecan Nano at 30°C with shaking, and the OD_{600} was recorded every 5 minutes. Samples
487 were run in biological triplicate and technical duplicate.
488
489 **Enumeration of phages produced during infection**
490 Overnight *Cglu* cultures were subcultured 1:100 into LBG supplemented with 10 mM $CaCl_2$ and apra and grown
491 to midlog. Cultures were normalized to an OD_{600}=0.3 and phage was added at an MOI of 2.5 while inducing
492 expression of cloned plasmid genes with 0.1 mM IPTG and 1 mM theophylline. Infected cultures were then
493 incubated for 2 hours at 30°C. At 2 hours post-infection, 100 µl of each sample was collected and centrifuged for
494 3 minutes at 10,000xg to remove the unlysed cells. The supernatant was then tenfold diluted in SM buffer and
495 tittered via dribble plating. Briefly, 10 mL of LBG 0.5% agar were mixed with 10 mM $CaCl_2$, 1 mM theophylline,
496 0.1 mM IPTG and a midlog *lysZ* complement host. This mixture was poured into a petri dish, allowed to solidify
497 under flame, and 10 µl of phage dilutions were then dribbled across the top of the solidified plate and dried under
498 flame. Plates were then incubated overnight at 30°C and plaques were enumerated the next day.
499
500 **Phage-infected *Cglu* microscopy**
501 Overnight *Cglu* cultures were diluted 1:100 into LBG supplemented with 10 mM $CaCl_2$ and grown to midlog.
502 Phage was added at an MOI of 10 and allowed 30 minutes for adsorption at 30°C with aeration. Infected cells
503 were then spotted onto an 2% LBG agarose pad supplemented with 10 mM $CaCl_2$ and imaged on a Nikon Ti-E
504 inverted widefield microscope with a motorized stage, a perfect focus system, and a 1.45 NA Plan Apo ×100 Ph3
505 DM objective lens with Cargille Type 37 immersion oil. Images were acquired with an Andor Zyla 4.2 Plus sCMOS

506 camera (65 nm pixel size) using Nikon Elements acquisition software (v5.10) and rendered for publication with
507 Fiji.
508
509 **Suppressor isolation and sequencing**
510 WT *Cglu* containing the ^{Cog}*lysZ* expression plasmid were grown overnight in the presence of antibiotics. Cultures
511 were serially tenfold diluted and 100 µl of the dilutions were plated onto BHIS agar plates supplemented with 0.1
512 mM IPTG, 1 mM theophylline, and apra. Plates were incubated for two days at 30ºC. Individual colonies were
513 patched onto BHI plates with or without 0.008% SDS. Colonies that failed to grow on SDS but grew successfully
514 on BHIS were then grown up in LBG supplemented with 10 mM $CaCl_2$ over-day along with a WT control. Then,
515 200 µl of these cultures were used to seed lawns for a phage spot assay as described above and incubated
516 overnight. *Cglu* suppressors that gained susceptibility to Cog Δ*lysZ* plaque formation were further purified and
517 their genomic DNA (gDNA) was isolated. Briefly, overnight cultures were harvested and incubated with 50 mM
518 EDTA and 1 mg/ml lysozyme at 37ºC for 30 minutes to remove the cell wall. Following lysozyme treatment, the
519 gDNA was extracted using the Promega Wizard DNA Extraction Kit and sent to the Microbial Genome
520 Sequencing Center in Pittsburgh, PA (now named SeqCenter). Mutational analysis was performed using the
521 breseq pipeline[41] and Geneious Prime Workbench, and the results were validated using Sanger sequencing.
522
523 **Lipomannan and lipoarabinomannan analysis**
524 Overnight cultures of *Cglu* were grown in BHIS supplemented with apra, 1mM theo and 0.01mM IPTG. Samples
525 were normalized to an OD_{600}~5 and 1mL was pelleted and resuspend in PBS and Laemmli buffer. Samples were
526 then boiled at 100ºC for 25 minutes and run on a 4-20% TGX gel. LM and LAM were then stained using the ProQ
527 Emeraled 300 Lipopolysaccharide Gel Stain Kit (Thermo Scientific) using standard protocols.
528
529 **Bioinformatics**
530 Putative *lysZ*-like alleles were identified through analysis of lysis cassettes of Actinophages available on
531 PhagesDB[42]. Representative phages from different clusters were arbitrarily chosen and visualized with
532 Pharmerator[43]. Genes proximal to the predicted endolysin(s) as well as genes at the end of the structural
533 modules were screened for predicted TM domains with DeepTMHMM[44]. Functional predictions were made with
534 HHPred and Foldseek[45] based on Alphafold2[46] generated models. Graphs were created with GraphPad Prism
535 and cartoons and figures were prepared in Adobe Illustrator.
536

537 **REFERENCES**

538 1. Cahill, J. & Young, R. Phage Lysis: Multiple Genes for Multiple Barriers. *Adv. Virus Res.* **103**, 33–70
539 (2019).
540 2. Gründling, A., Manson, M. D. & Young, R. Holins kill without warning. *Proc. Natl. Acad. Sci. U. S. A.* **98**,
541 9348–9352 (2001).
542 3. Summer, E. J. *et al.* Rz/Rz1 Lysis Gene Equivalents in Phages of Gram-negative Hosts. *J. Mol. Biol.* **373**,
543 1098–1112 (2007).
544 4. Berry, J., Summer, E. J., Struck, D. K. & Young, R. The final step in the phage infection cycle: The Rz and
545 Rz1 lysis proteins link the inner and outer membranes. *Mol. Microbiol.* **70**, 341–351 (2008).
546 5. Rajaure, M., Berry, J., Kongari, R., Cahill, J. & Young, R. Membrane fusion during phage lysis. *Proc. Natl.*
547 *Acad. Sci. U. S. A.* **112**, 5497–5502 (2015).
548 6. Berry, J., Rajaure, M., Pang, T. & Young, R. The spanin complex is essential for lambda lysis. *J. Bacteriol.*
549 **194**, 5667–5674 (2012).
550 7. Sun, J., Rutherford, S. T., Silhavy, T. J. & Huang, K. C. Physical properties of the bacterial outer
551 membrane. *Nat. Rev. Microbiol.* **20**, 236–248 (2022).
552 8. Dulberger, C. L., Rubin, E. J. & Boutte, C. C. The mycobacterial cell envelope - a moving target. *Nat. Rev.*
553 *Microbiol.* **18**, 47–59 (2020).
554 9. Gil, F. *et al.* The lytic cassette of mycobacteriophage Ms6 encodes an enzyme with lipolytic activity.
555 *Microbiology* **154**, 1364–1371 (2008).
556 10. Payne, K., Sun, Q., Sacchettini, J. & Hatfull, G. F. Mycobacteriophage Lysin B is a novel
557 mycolylarabinogalactan esterase. *Mol. Microbiol.* **73**, 367–381 (2009).
558 11. Alva, V., Nam, S.-Z., Söding, J. & Lupas, A. N. The MPI bioinformatics Toolkit as an integrative platform
559 for advanced protein sequence and structure analysis. *Nucleic Acids Res.* **44**, W410–W415 (2016).
560 12. Saier, M. H., Tran, C. V. & Barabote, R. D. TCDB: the Transporter Classification Database for membrane
561 transport protein analyses and information. *Nucleic Acids Res.* **34**, 181–186 (2006).
562 13. Portevin, D. *et al.* A polyketide synthase catalyzes the last condensation step of mycolic acid biosynthesis
563 in mycobacteria and related organisms. *Proc. Natl. Acad. Sci. U. S. A.* **101**, 314–319 (2004).
564 14. McKitterick, A. C. & Bernhardt, T. G. Phage resistance profiling identifies new genes required for
565 biogenesis and modification of the corynebacterial cell envelope. *Elife* **11**, e79981 (2022).
566 15. Patterson, J. H., Waller, R. F., Jeevarajah, D., Billman-Jacobe, H. & McConville, M. J. Mannose
567 metabolism is required for mycobacterial growth. *Biochem. J.* **372**, 77–86 (2003).
568 16. McCarthy, T. R. *et al.* Overexpression of Mycobacterium tuberculosis manB, a phosphomannomutase
569 that increases phosphatidylinositol mannoside biosynthesis in Mycobacterium smegmatis and
570 mycobacterial association with human macrophages. *Mol. Microbiol.* **58**, 774–790 (2005).
571 17. Gurcha, S. S. *et al.* Ppm1, a novel polyprenol monophosphomannose synthase from Mycobacterium
572 tuberculosis. *Biochem. J.* **365**, 441–450 (2002).
573 18. Gibson, K. J. C. *et al.* Disruption of Cg-Ppm1, a Polyprenyl Monophosphomannose Synthase, and the

574 Generation of Lipoglycan-less Mutants in Corynebacterium glutamicum. *J. Biol. Chem.* **278**, 40842–40850
575 (2003).
576 19. Ning, B. & Elbein, A. D. Purification and properties of mycobacterial GDP-mannose pyrophosphorylase.
577 *Arch. Biochem. Biophys.* **362**, 339–345 (1999).
578 20. Lea-Smith, D. J. *et al.* Analysis of a new mannosyltransferase required for the synthesis of
579 phosphatidylinositol mannosides and lipoarbinomannan reveals two lipomannan pools in
580 corynebacterineae. *J. Biol. Chem.* **283**, 6773–6782 (2008).
581 21. Mishra, A. K. *et al.* Identification of a novel α(1→6) mannopyranosyltransferase MptB from
582 Corynebacterium glutamicum by deletion of a conserved gene, NCgl1505, affords a lipomannan- and
583 lipoarabinomannan-deficient mutant. *Mol. Microbiol.* **68**, 1595–1613 (2008).
584 22. Mishra, A. K. *et al.* Identification of an α(1→6) mannopyranosyltransferase (MptA), involved in
585 Corynebacterium glutamicum lipomanann biosynthesis, and identification of its orthologue in
586 Mycobacterium tuberculosis. *Mol. Microbiol.* **65**, 1503–1517 (2007).
587 23. Mishra, A. K. *et al.* Lipoarabinomannan biosynthesis in Corynebacterineae: The interplay of two α(1→2)-
588 mannopyranosyltransferases MptC and MptD in mannan branching. *Mol. Microbiol.* **80**, 1241–1259
589 (2011).
590 24. Mahne, M., Tauch, A., Pühler, A. & Kalinowski, J. The Corynebacterium glutamicum gene pmt encoding
591 a glycosyltransferase related to eukaryotic protein-O-mannosyltransferases is essential for glycosylation
592 of the resuscitation promoting factor (Rpf2) and other secreted proteins. *FEMS Microbiol. Lett.* **259**, 226–
593 233 (2006).
594 25. Sparks, I. L. *et al.* Lipoarabinomannan mediates localized cell wall integrity during division in
595 mycobacteria. *Nat. Commun.* **15**, 8–10 (2024).
596 26. Guan, S., Bastin, D. A. & Verma, N. K. Functional analysis of the O antigen glucosylation gene cluster of
597 Shigella flexneri bacteriophage SfX. *Microbiology* **145**, 1263–1273 (1999).
598 27. Sher, J. W., Lim, H. C. & Bernhardt, T. G. Global phenotypic profiling identifies a conserved actinobacterial
599 cofactor for a bifunctional pbp-type cell wall synthase. *Elife* **9**, e54761 (2020).
600 28. Puech, V. *et al.* Structure of the cell envelope of corynebacteria: Importance of the non-covalently bound
601 lipids in the formation of the cell wall permeability barrier and fracture plane. *Microbiology* **147**, 1365–1382
602 (2001).
603 29. Zuber, B. *et al.* Direct visualization of the outer membrane of mycobacteria and corynebacteria in their
604 native state. *J. Bacteriol.* **190**, 5672–5680 (2008).
605 30. D'Elia, M. A. *et al.* Lesions in teichoic acid biosynthesis in Staphylococcus aureus lead to a lethal gain of
606 function in the otherwise dispensable pathway. *J. Bacteriol.* **188**, 4183–4189 (2006).
607 31. Jorgenson, M. A., Kannan, S., Laubacher, M. E. & Young, K. D. Dead-end intermediates in the
608 enterobacterial common antigen pathway induce morphological defects in Escherichia coli by competing
609 for undecaprenyl phosphate. *Mol. Microbiol.* **100**, 1–14 (2016).
610 32. Jorgenson, M. A. & Young, K. D. Interrupting biosynthesis of O antigen or the lipopolysaccharide core

611 produces morphological defects in Escherichia coli by sequestering undecaprenyl phosphate. *J. Bacteriol.*
612 **198**, 3070–3079 (2016).
613 33. Rojas, E. R. *et al.* The outer membrane is an essential load-bearing element in Gram-negative bacteria.
614 *Nature* **559**, 617–621 (2018).
615 34. Breukink, E. *et al.* Use of the cell wail precursor lipid II by a pore-forming peptide antibiotic. *Science (80-.*
616 *).* **286**, 2361–2364 (1999).
617 35. Ravasi, P., Peiru, S., Gramajo, H. & Menzella, H. G. Design and testing of a synthetic biology framework
618 for genetic engineering of Corynebacterium glutamicum. *Microb. Cell Fact.* **11**, 147 (2012).
619 36. Topp, S. *et al.* Synthetic riboswitches that induce gene expression in diverse bacterial species. *Appl.*
620 *Environ. Microbiol.* **76**, 7881–7884 (2010).
621 37. Okibe, N., Suzuki, N., Inui, M. & Yukawa, H. Efficient markerless gene replacement in Corynebacterium
622 glutamicum using a new temperature-sensitive plasmid. *J. Microbiol. Methods* **85**, 155–163 (2011).
623 38. Hart, E. M., Lyerly, E. & Bernhardt, T. G. The conserved σD envelope stress response monitors multiple
624 aspects of envelope integrity in corynebacteria. *PLoS Genet.* **20**, (2024).
625 39. Filsinger, G. T. *et al.* A diverse single-stranded DNA-annealing protein library enables efficient genome
626 editing across bacterial phyla. *Proc. Natl. Acad. Sci.* **122**, e2414342122 (2025).
627 40. Jiang, Y. *et al.* CRISPR-Cpf1 assisted genome editing of Corynebacterium glutamicum. *Nat. Commun.* **8**,
628 1–11 (2017).
629 41. Deatherage, D. E. & Barrick, J. E. Identification of Mutations in Laboratory-Evolved Microbes from Next-
630 Generation Sequencing Data Using breseq. *Methods Mol Bio* **1151**, 188 (2014).
631 42. Russell, D. A. & Hatfull, G. F. PhagesDB: The actinobacteriophage database. *Bioinformatics* **33**, 784–786
632 (2017).
633 43. Cresawn, S. G. *et al.* Phamerator: A bioinformatic tool for comparative bacteriophage genomics. *BMC*
634 *Bioinformatics* **12**, (2011).
635 44. Hallgren, J. *et al.* DeepTMHMM predicts alpha and beta transmembrane proteins using deep neural
636 networks. *bioRxiv* 2022.04.08.487609 (2022).
637 45. Kempen, M. van *et al.* Foldseek: fast and accurate protein structure search. *bioRxiv* 2022.02.07.479398
638 (2022) doi:10.1038/s41587-023-01773-0.
639 46. Mirdita, M. *et al.* ColabFold: making protein folding accessible to all. *Nat. Methods* **19**, 679–682 (2022).
640
641
642
643

644 **FIGURES**

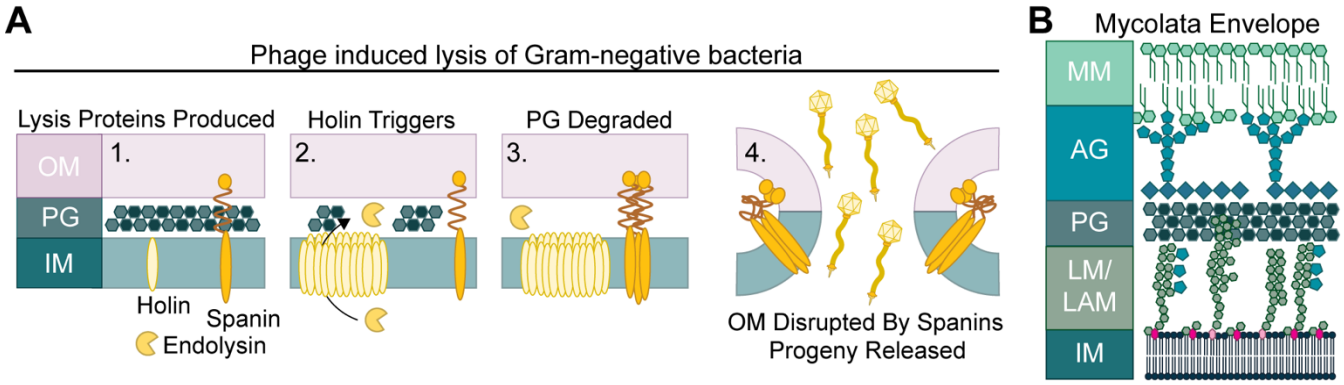

645

646 **Figure 1. Gram-negative cell lysis and the mycolata envelope. A**. Cartoon detailing the steps of phage-
647 induced lysis of a Gram-negative cell. (Step 1) Production of the phage lysis proteins: holin, endolysin, and
648 spanin. (2) Holin triggering leads to formation of large pores in the membrane that allow the endolysin to enter
649 the periplasmic space. (3) The endolysin degrades the peptidoglycan (PG) cell wall, allowing spanin
650 multimerization. (4) Multimerized spanins induce fusion of the inner membrane (IM) and outer membrane (OM),
651 leading to lysis and phage progeny release. **B**. Diagram of the mycolata envelope that surrounds bacteria of the
652 Mycobacteriales order. IM, inner membrane; LM/LAM, lipomannan and lipoarabinomannan; PG, peptidoglycan;
653 AG, arabinogalactan; MM, mycomembrane; OM, outer membrane.

654

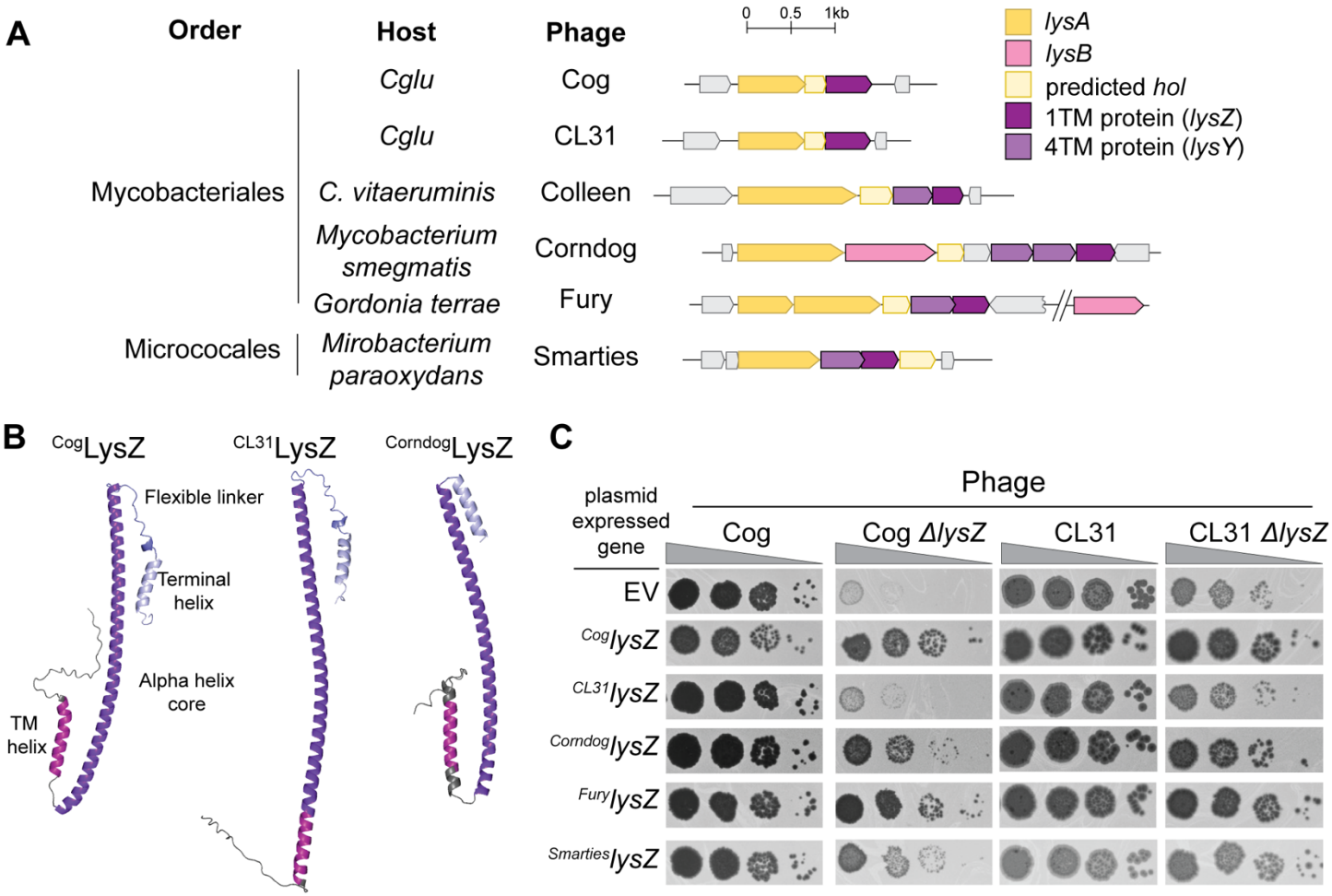

Figure 2. LysZ is required for efficient corynephage plaque formation. A. Diagrams of lysis cassettes from the corynephage Cog and other actinophages. The genes encoded in the cassettes are: *lysA* endolysin, *lysB* esterase, *hol* holin, and predicted lysis genes *lysZ* and *lysY*. **B**. Alphafold2 models of LysZ structures from the indicated phages with structural features highlighted. **C**. Tenfold serial dilutions of the indicated phages were spotted on a lawn of wild-type *Cglu* harboring the indicated gene on a multicopy plasmid under control of an IPTG-inducible *tac* promoter (P_{tac}) and a modified *riboE1* riboswitch (*riboE1**) that allows translation in the presence of the inducer theophylline. Expression was induced by the addition of IPTG (100 μM) and theophylline (1 mM) to the soft agar. EV denotes empty vector.

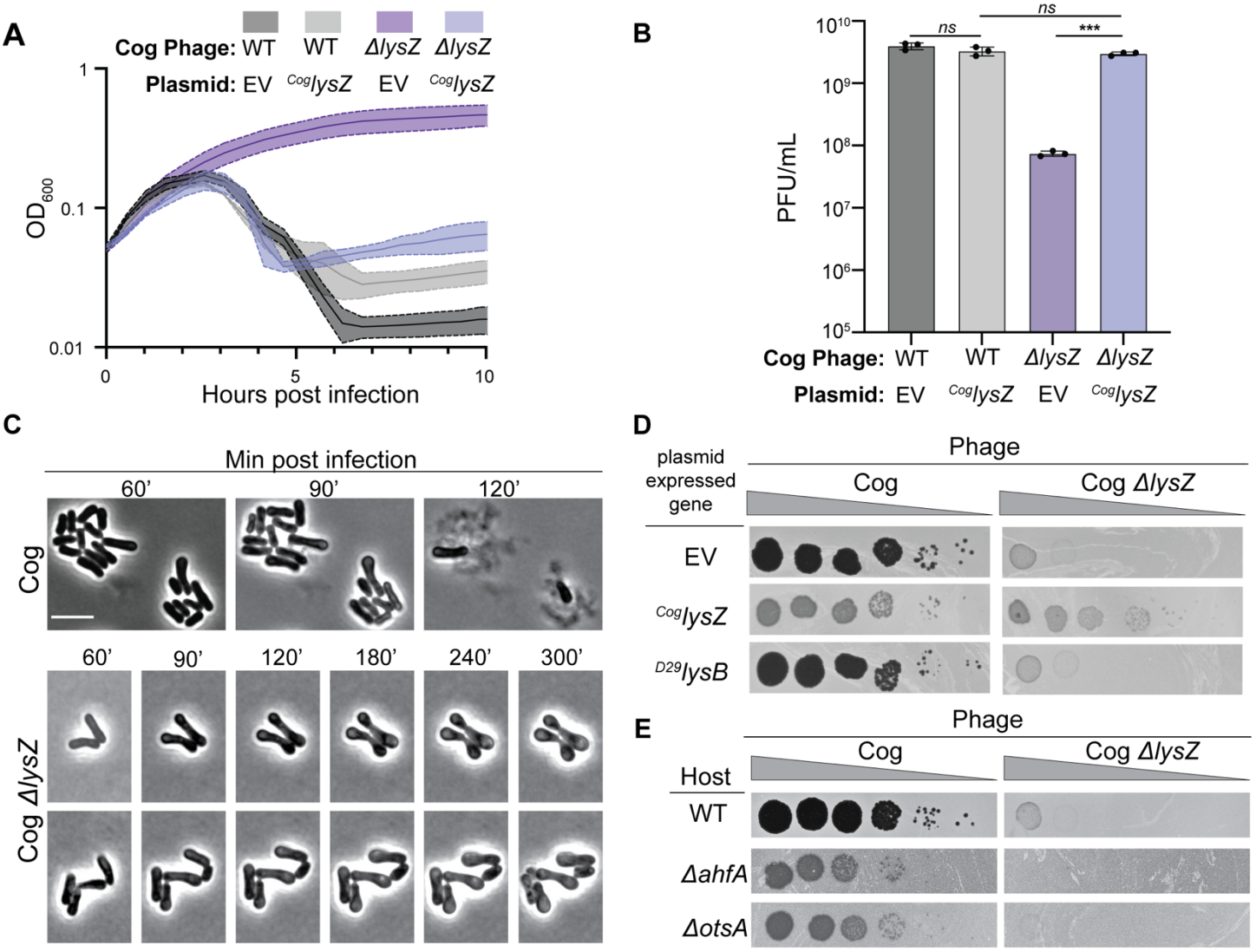

Figure 3. LysZ is needed to induce host cell lysis. A. Cells of *Cglu* harboring the indicated expression plasmid were infected with the indicated phage at an MOI of 2.5. Expression of the indicated genes was induced with IPTG (100 μM) and theophylline (1 mM) at the time of infection. Growth of the infected culture was followed by monitoring OD_{600}. Shaded regions indicate standard deviation, and solid lines indicate the mean from three independent experiments. **B.** Enumeration of phages released 120 minutes post infection of the listed strains with the listed phages. Expression of the indicated genes was induced with IPTG (100 μM) and theophylline (1 mM) at the time of infection. Dots represent individual data points, bar heights represent the mean, and error bars indicate standard deviation of three independent experiments. Significance was determined by a two-tailed t test. *ns,* not significant; ***p<0.0001. **C**. Time-lapse microscopy of *Cglu* infected at an MOI of 10 with the indicated Cog variant and immobilized on agarose pads. Images of *Cglu* infected with Cog *ΔlysZ* show two representative sets of cells. Bar equals 5 μm. **D.** Tenfold serial dilutions of the indicated phages were spotted on a lawn of wild-type *Cglu* harboring the indicated gene on a multicopy plasmid induced as in **Fig. 2**. **E.** Tenfold serial dilutions of the indicated phages were spotted on lawns of the indicated *Cglu* hosts.

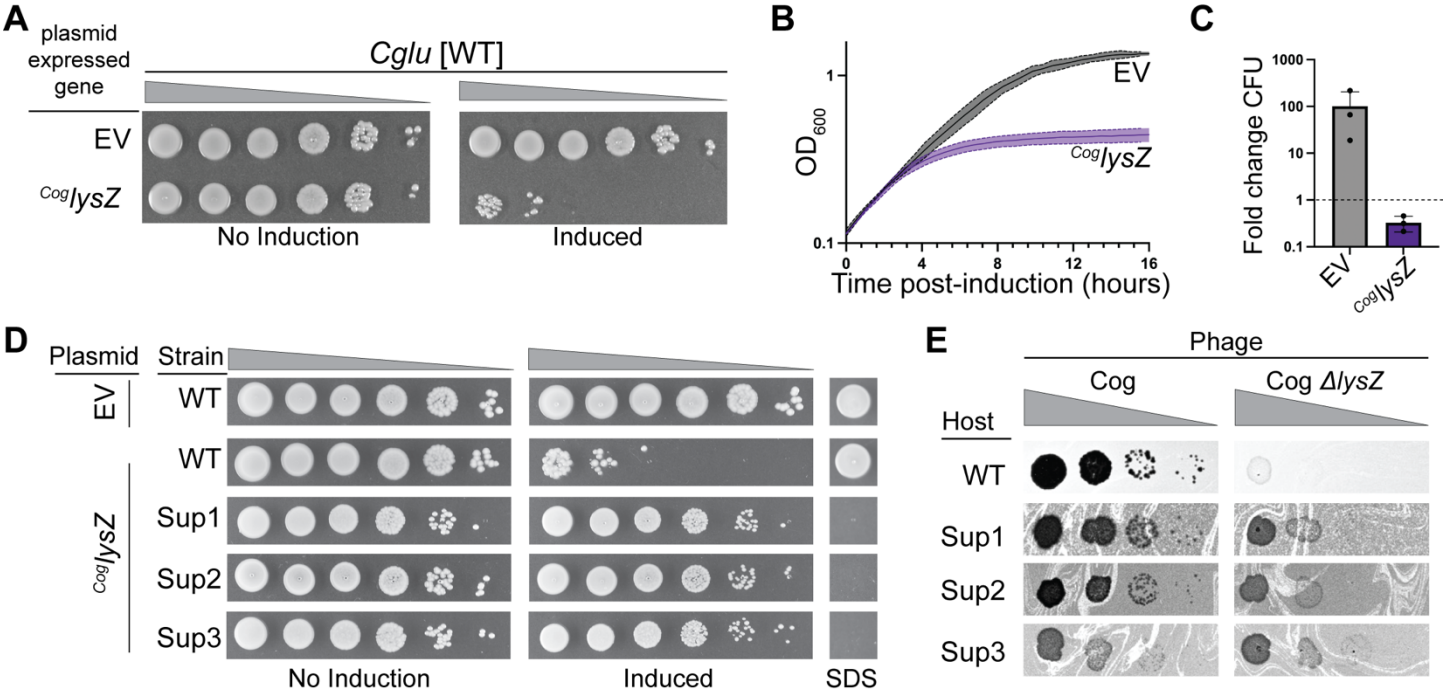

Figure 4. ^{Cog}LysZ overexpression is lethal. A. Wild-type *Cglu* with an empty vector (EV) or ^{Cog}*lysZ* containing expression plasmid were serially diluted and plated on agar with and without IPTG (100 μM) and theophylline (1 mM) for induction of gene expression from the plasmid. **B**. Growth of the same strains in (**A**) was followed by monitoring culture OD_{600} after induction with IPTG (100 μM) and theophylline (1 mM). Shaded regions indicate standard deviation, and solid lines indicate the mean from three independent experiments. **C.** Change in colony forming units (CFU) of the indicated strains after overnight induction as in (**C**). Dots represent individual data points, bar heights represent the mean, and error bars indicate standard deviation of three independent experiments. Significance was determined by a two-tailed t test. **D.** Tenfold dilutions of the indicated *Cglu* expression strain spotted with or without inducers as in (**A**). To the right, SDS sensitivity was monitored. Cultures normalized to OD_{600} = 1 were spotted on agar containing 0.0075% SDS. Sup1 = *cgp_0855*::*IS*, Sup2 = *manB*, and Sup3 = *ppmC*. **E.** Tenfold serial dilutions of the indicated phages were spotted on lawns of the indicated *Cglu* hosts.

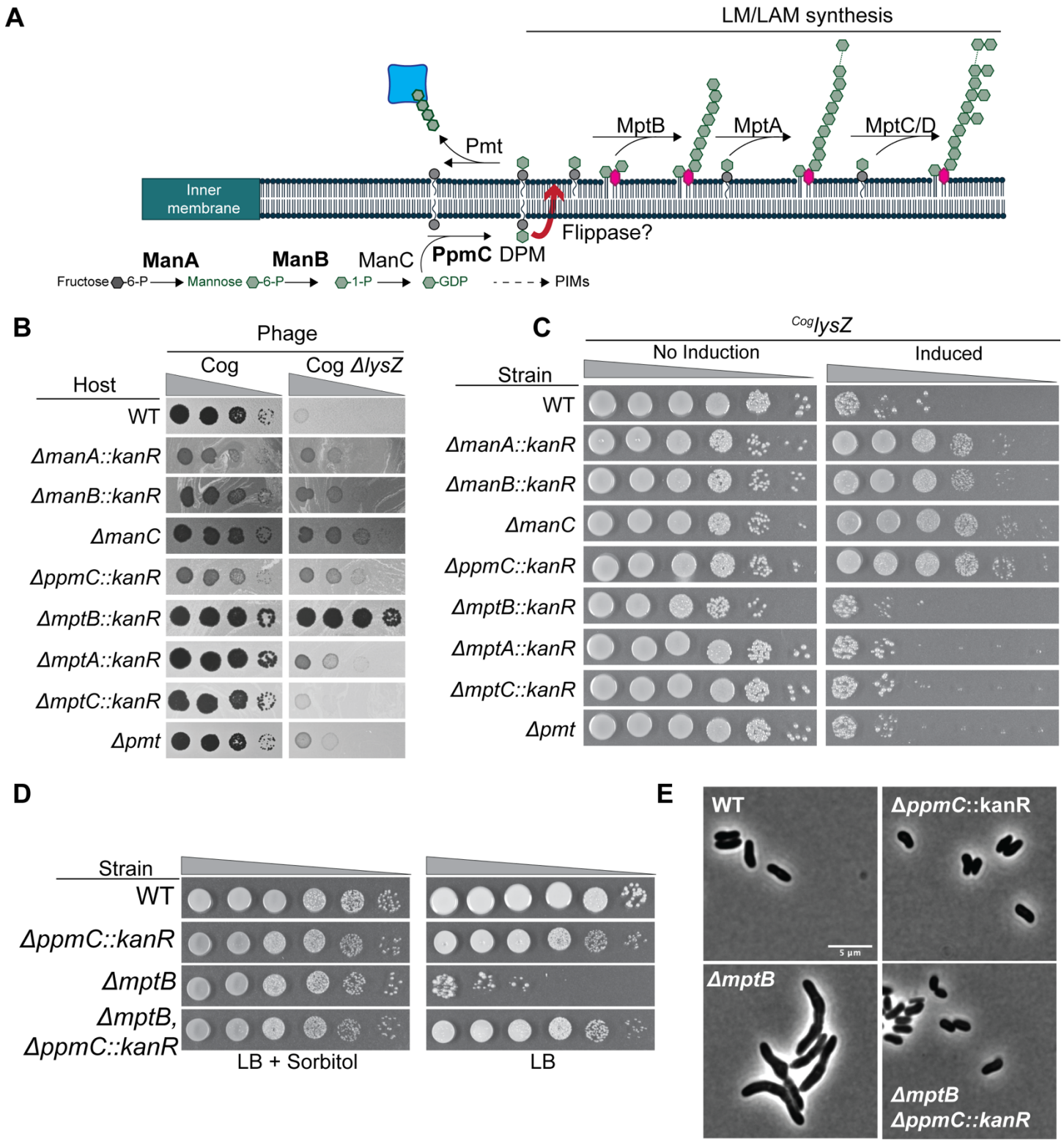

Figure 5. LysZ is dispensable host lysis in strains lacking LM/LAM. A. Diagram of the LM/LAM biogenesis pathway. See text for details. Enzymes highlighted in bold indicate steps in the pathway affected by suppressor mutations that alleviate ^{Cog}*lysZ* toxicity. **B**. Tenfold dilutions of the indicated phage variants spotted on lawns of the indicated mutant *Cglu* hosts. **C.** Tenfold dilutions of the indicated strains harboring the ^{Cog}*lysZ* expression plasmid were plated with and without inducer as in **Fig. 4A**. **D**. Tenfold dilutions of the indicated *Cglu* strains

703 spotted on LB agar with or without sorbitol (9.1%) as indicated. **E**. Phase contrast images of the indicated strains.
704 Bar equals 5 μm.
705

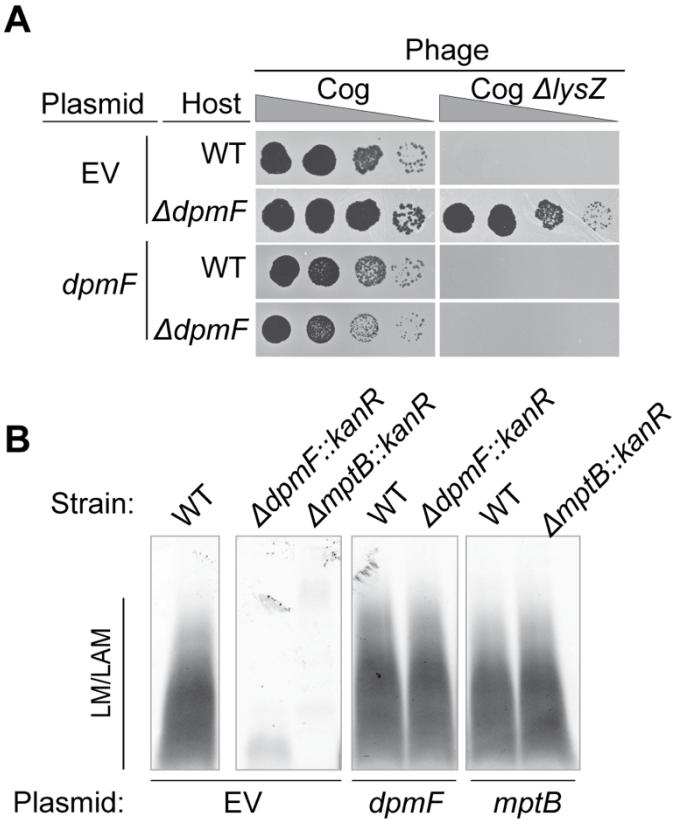

Figure 6. Evidence that *dpmF* encodes the DPM flippase. A. Tenfold dilutions of the indicated phage spotted on lawns of hosts containing the indicated expression plasmid. Expression was induced with IPTG (10 μM) and theophylline (1 mM) in cultures for approximately 6 hours before lawns were prepared and induction was maintained in the soft agar. **B**. LM/LAM was harvested from overnight cultures of the indicated strains and analyzed by SDS-PAGE and ProQ Emerald staining. Overnight cultures were induced with IPTG and theophylline as in **A**.

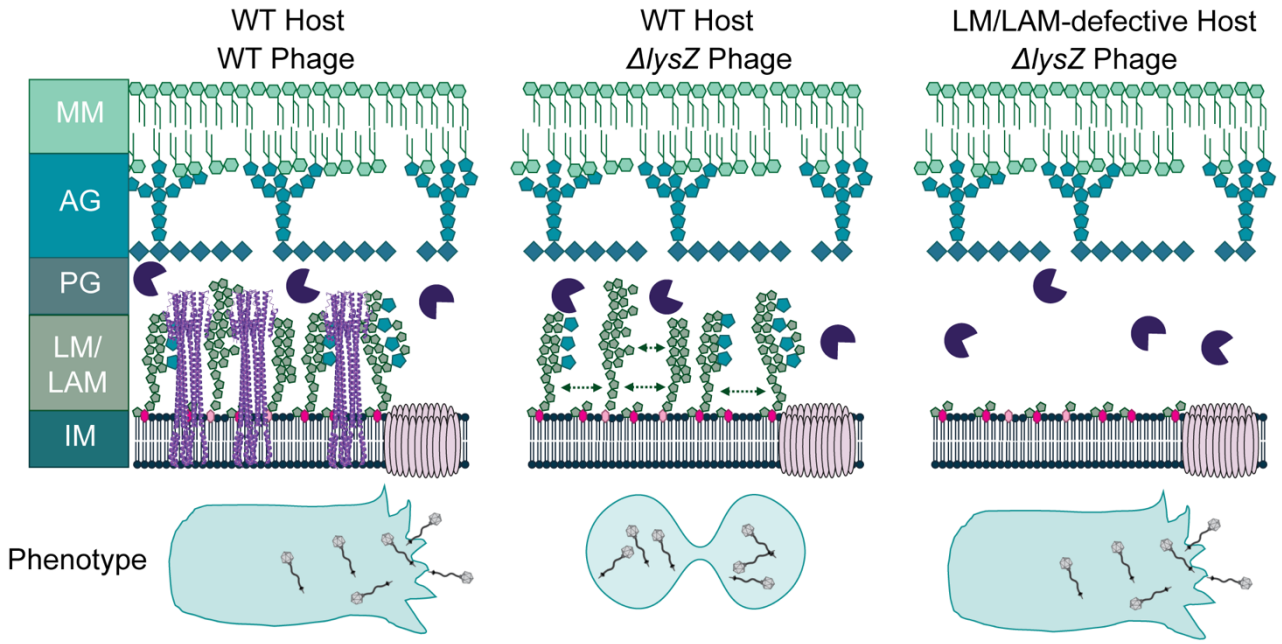

714

715 **Figure 7. Model for LysZ function. Left.** LysZ functions to disrupt interactions between LM/LAM polymers to
716 assist host cell lysis following holin triggering and PG degradation by the endolysin. **Middle.** Infection of wild-
717 type *Cglu* with a phage lacking LysZ results in lysis failure due to the stabilizing properties of LM/LAM lipoglycans.
718 **Right.** Infections of cells lacking LM/Lam do not require LysZ to induce host cell lysis.

719

Supplemental Material for:

Bacteriophages target membrane-anchored glycopolymers to promote host cell lysis and progeny release

Authors: Amelia C. McKitterick[1,2,3*], Evan W. Lyerly[1,2], and Thomas G. Bernhardt[1,2*]

Affiliations:
[1]Department of Microbiology
Harvard Medical School
Boston, MA 02115

[2]Howard Hughes Medical Institute

[3]Department of Microbiology
University of Massachusetts Chan Medical School
Worcester, MA 01605

*To whom correspondence should be addressed
Thomas G. Bernhardt
Harvard Medical School
Department of Microbiology
Boston, MA 02115
e-mail: thomas_bernhardt@hms.harvard.edu

or

Amelia C. McKitterick
University of Massachusetts Chan Medical School
Department of Microbiology
Worcester, MA 01605
e-mail: amelia.mckitterick@umassmed.edu

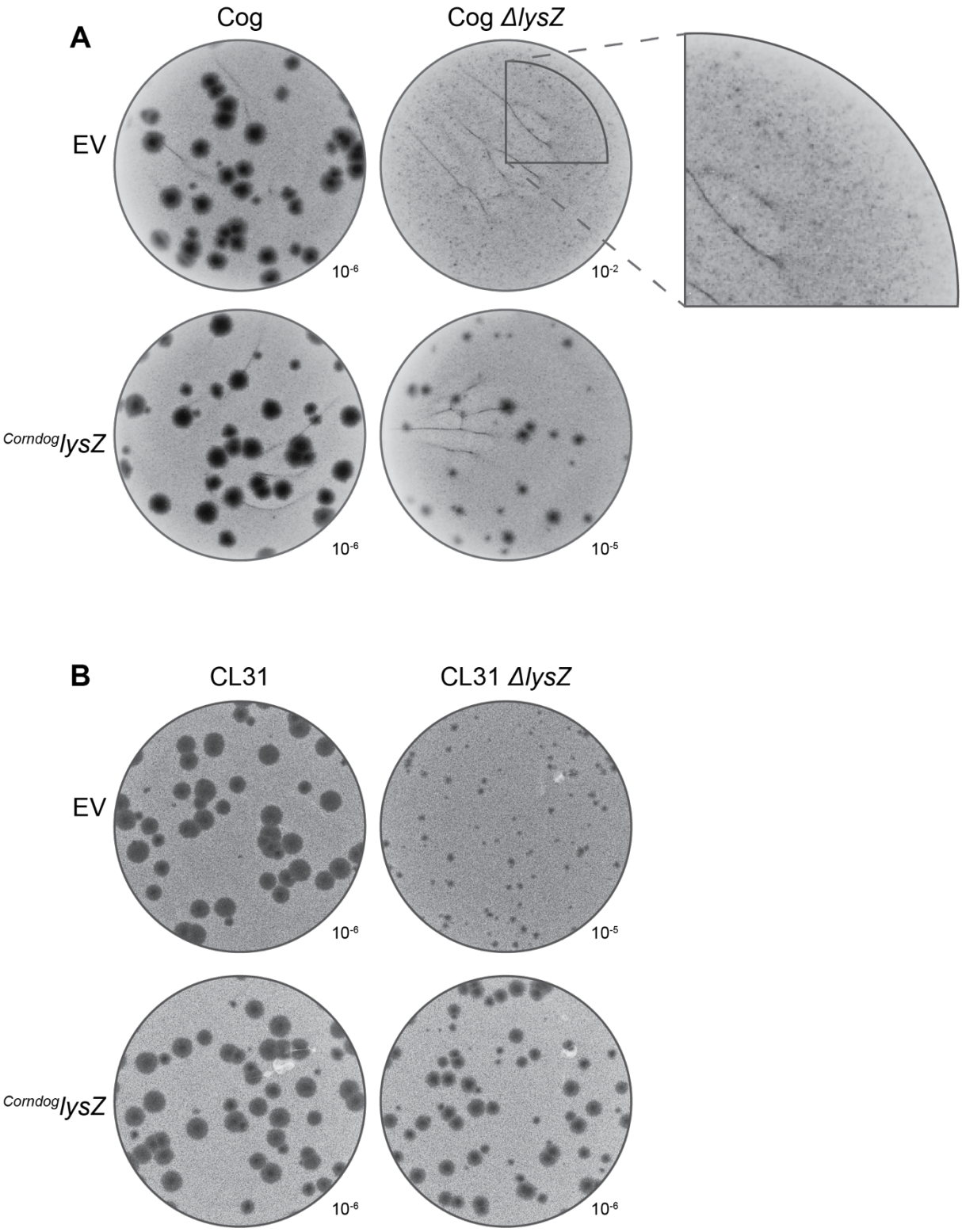

Figure S1. Phages lacking LysZ have defects in plaque formation. A, Listed dilutions of the indicated phages infecting the indicated *Cglu* expression strain in 0.25% top agar. Inset shows zoomed in view of Cog ΔlysZ plaques. Genes were induced with IPTG (100 μM) and theophylline (1 mM) in the soft agar. **B,** Listed dilutions of the indicated phages infecting the indicated *Cglu* expression strain in 0.5% top agar. Genes were induced with IPTG (100 μM) and theophylline (1 mM) in the soft agar.

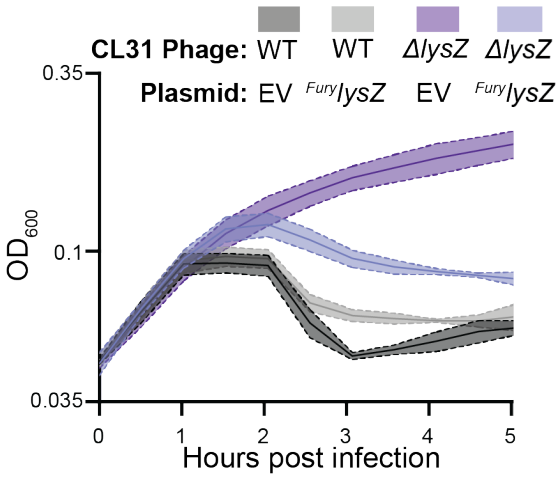

Figure S2. Lysis kinetics of CL31 phage. Cells of *Cglu* harboring the indicated expression plasmid were infected with the indicated phage at an MOI of 2.5. Expression of the indicated genes was induced with IPTG (100 μM) and theophylline (1 mM) at the time of infection. Growth of the infected culture was followed by monitoring OD_{600}. Shaded regions indicate standard deviation, and solid lines indicate the mean from three independent experiments.

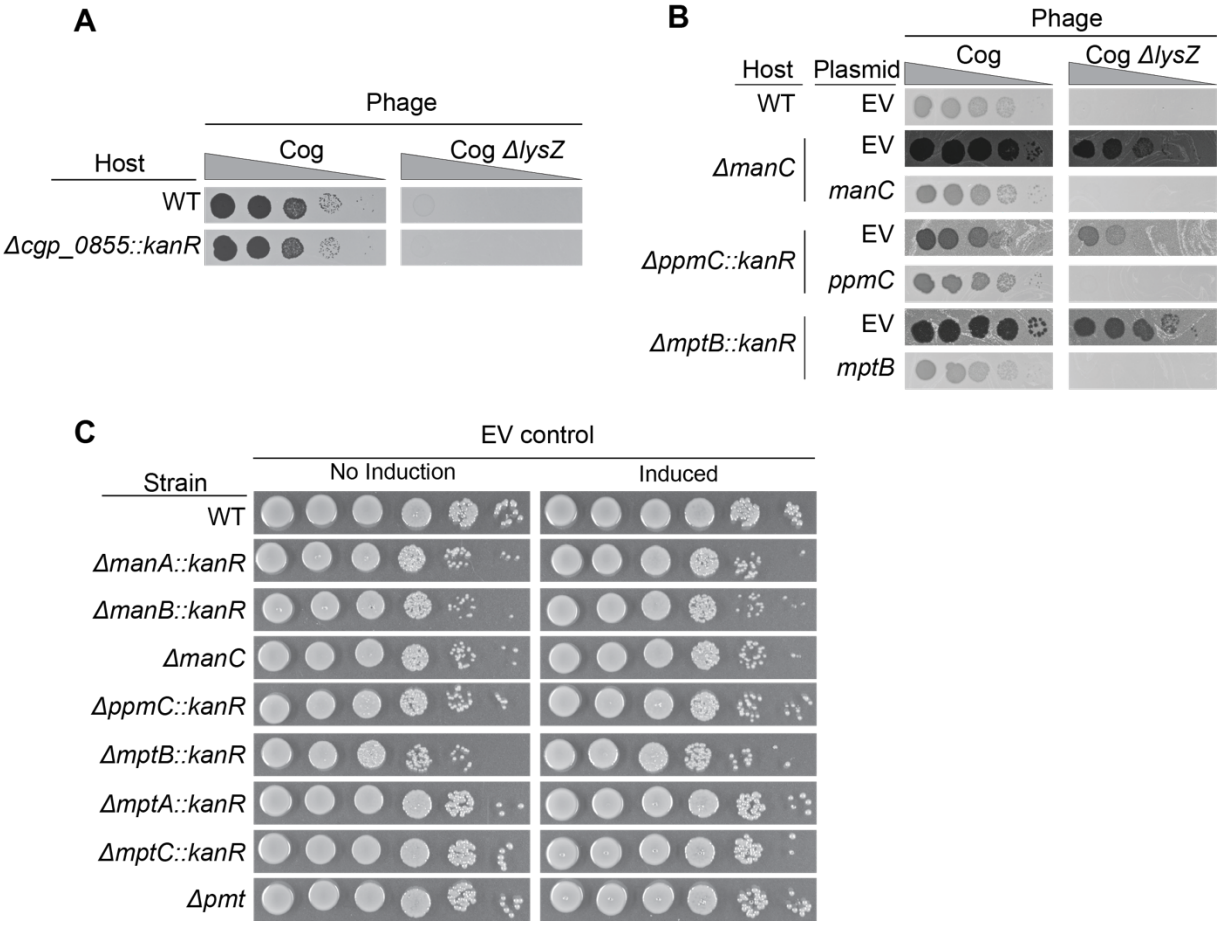

Figure S3. Complementation and other controls. A. Tenfold dilutions of the indicated phage variants spotted on lawns of the indicated mutant *Cglu* hosts. **B.** Tenfold dilutions of the indicated phage variants spotted on lawns of the indicated mutant *Cglu* hosts harboring the indicated expression plasmids. The indicated genes were under control of P_{tac} and riboE1*. Induction was performed in liquid cultures for approximately 6 hours before plating with IPTG (100 μM) and theophylline (1 mM) maintained in the top agar. **C**. Tenfold dilutions of the indicated *Cglu* strains harboring the empty expression vector were grown on agar with no inducer or with IPTG (100 μM) and theophylline (1 mM).

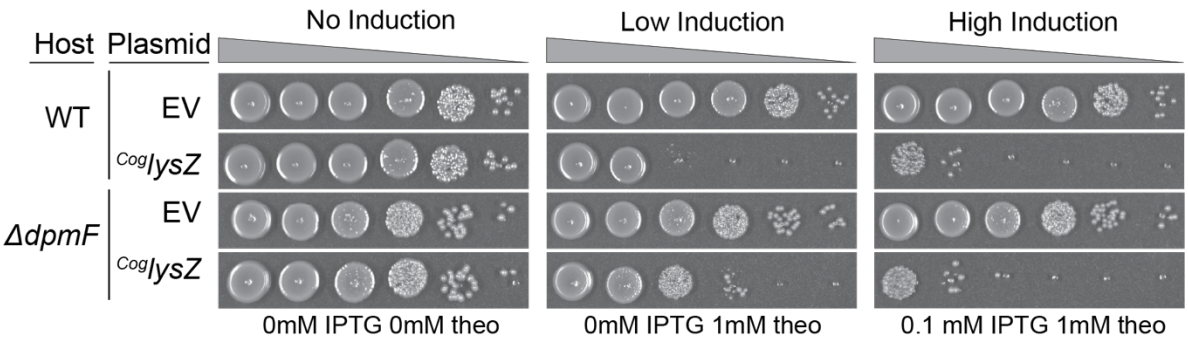

Figure S4. **Intermediate sensitivity of *ΔdpmF* cells to *LysZ*.** Tenfold dilutions of the indicated *Cglu* strains harboring the empty or ^{Cog}*lysZ* expression vector were grown on agar with no inducer or with low (IPTG = 10 μM), theophylline = 1 mM) or high (IPTG = 100 μM), theophylline = 1 mM) concentrations of inducer.

SUPPLEMENTARY MOVIES

Movie 1. Lysis of *Cglu* infected with WT Cog. Cells were infected with Cog at an MOI = 10. After 30 minutes for adsorption, infected cells were spotted onto an agarose pad for observation. Images were captured every 15 seconds.

Movie 2. Lysis of *Cglu* infected with Cog *ΔlysZ* – site 1. Cells were infected with Cog *ΔlysZ* infected and imaged as in Movie 1 except that images were captured every 1 minute.

Movie 3. Lysis of *Cglu* infected with Cog *ΔlysZ* - site 2. Cells were infected with Cog *ΔlysZ* infected and imaged as in Movie 1 except that images were captured every 1 minute.

SUPPLEMENTARY TABLES

Table S1. *LysZ* suppressors.

Isolate	Position	Mutation	Annotation	Gene	Description
Suppressor 1	788,382	transposition		*cgp_0855*	transposon insertion in cgp_0855, upstream of *manA*
Suppressor 2	786,820	A→C	D248A (GAT→GCT)	*pmmA*	phosphomannomutase
Suppressor 2	980,716	C→G	A187P (GCA→CCA)	*cgp_1053*	putative transcriptional regulator, TetR-family
Suppressor 2	1,668,571	G→T	P280Q (CCA→CAA)	*gap*	glyceraldehyde-3-phosphate dehydrogenase (GAPDH)
Suppressor 3	1,547,187	G→A	Q190* (CAA→TAA)	*ppmC*	polyprenol-phosphate-mannose synthase domain 1

Table S2. Strains used in this study.

Strain	Name	Genotype	Ref.
DH5a (lpir)		*F– hsdR17 deoR recA1 endA1 phoA supE44 thi-1 gyrA96 relA1 Δ(lacZYA-argF)U169 ϕ80dlacZΔM15 ****add pir*	Gibco BRL
MB001	H#0060	MB001 (ATCC 13032 ΔCGP1 (cg1507-gp1524) ΔCGP2 (cg1746-1752) ΔCGP3 (cg1890-cg2071))	(1)
ΔahfA	H#2262	MB001 *ΔahfA* (*cgp_0475*)	(2)
ΔotsA	H#1666	MB001 *ΔotsA* (*cgp_2907*)	(2)
Suppressor 1	H#5306	MB001 pTGR5_SNP_riboE-Cog_gp25 apraR *cgp_0855* transposon insertion	This paper
Suppressor 2	H#5308	MB001 pTGR5_SNP_riboE-Cog_gp25 apraR; *pmmA* asp248ala; *cgp_1053* ala187pro; *gap* pro280gln	This paper
Suppressor 3	H#5307	MB001 pTGR5_SNP_riboE-Cog_gp25 apraR; *ppmC* Gln190*	This paper
Δcgp_0855::kanR	H#5365	MB001 *Δcgp0855::kanR lox*	This paper
ΔmanA::kanR	H#2559	MB001 *ΔmanA::kanR lox*	This paper
ΔmanB::kanR	H#3681	MB001 *ΔpmmA::kanR lox*	This paper
ΔmanC	H#3678	MB001 *ΔmanC*	This paper
ΔppmC::kanR	H#3679	MB001 *ΔppmC::kanR*	This paper
ΔdpmF::kanR	H#3680	MB001 *ΔmanA::kanR*	This paper
ΔdpmF	H#5406	MB001 *ΔmanA::lox*	This paper
ΔmptB::kanR	H#2439	MB001 *ΔmptB::kanR*	This paper
ΔmptB	H#5405	MB001 *ΔmptB::lox*	This paper
ΔmptB ΔppmC::kanR	H#5413	MB001 *ΔmptB::lox ΔppmC::kanR*	This paper
ΔmptB ΔdpmF::kanR	H#5102	MB001 *ΔmptB::lox ΔmanA::kanR*	This paper
ΔmptA::kanR	H#2438	MB001 *ΔmptA::kanR*	This paper
ΔmptC::kanR	H#2440	MB001 *ΔmptC::kanR*	This paper
Δpmt	H#2060	MB001 *Δpmt (cgp_1014)*	This paper

Table S3. Phages used in this study.

Isolate	Strain no	Genotype/notes	Ref.
Cog	ACMΦ008		(2)
Cog *ΔlysZ*	ACMΦ159	deletion of *lysZ* (*gp25)*	This paper
CL31	ACMΦ002		(2)
CL31 *ΔlysZ*	ACMΦ095	deletion of *lysZ (gp22*)	This paper

Table S4. Plasmids used in this study.

Construct name in paper	Plasmid	Genotype	Ref.
pCRE	pEWL89	pCRD206(ApraR)::P_{SOD}-*cre*	(3)
recombineering 1	pEWL054	pTGR5(CamR)::P_{tac}-*SSAP/SSB*	(3)
recomineering 2	pEWL103	pCRD206(ApraR)::P_{tac} riboE1-SSAP/SSB	(3)
pJYS3	pJYS3		(4)
pFSC	pFSC		(5)
P_{tac}-GFP	pTGR5	KanR, P_{tac}-*eGFP*, pGA1 mini replicon	(6)
pCRD206::*pmt*	pARP1	KanR, pCRD206 derivative containing an insert covering upstream and downstream of *cgp_1014* (*pmt*)	This paper
pCRD206::*ΔmanC*	pACM407	KanR, pCRD206 derivative containing an insert covering upstream and downstream of *cgp_0422* (*manC*)	This paper
P_{SOD}_*cas12*	pEWL001	KanR, pK-PIM derivative encoding P_{SOD}_riboE1-Cas12	This paper
P_{SOD} _Cas12_P_{tac}_anti-^{CL31}*lysZ*_spacer	pACM363	CmR, pTGR5 derivative encoding the CRISPR-Cas12 system and a spacer to target CL31 *lysZ*	This paper
P_{SOD} _Cas12_ P_{tac} _anti-^{Cog}*lysZ*_spacer	pACM351	CmR, pTGR5 derivative encoding the CRISPR-Cas12 system and a spacer to target Cog *lysZ*	This paper
P_{SOD} _Cas12_ P_{tac} _CRISPR-array	pEWL018	CmR, pTGR5 derivative encoding P_{SOD}_Cas12 and P_{tac} _CRISPR array with BsaI digest sites for spacer editing	This paper
P_{SOD} _dCas12_P_{tac}_CRISPR-array	pEWL013	CmR, pTGR5 derivative encoding P_{SOD}_dCas12 and P_{tac} _CRISPR array with BsaI digest sites for spacer editing	This paper
P_{tac}_*riboE_*manA*	pACM964	ApraR, pTGR5 derivative encoding P_{tac}_*riboE1-*manA*	This paper
P_{tac}_*riboE_^{CL31}*lysZ*	pACM490	ApraR, pTGR5 derivative encoding P_{tac}_*riboE1-^{CL31}*lysZ* *(gp22)*	This paper
P_{tac}_*riboE_^{Cog}*lysZ*	pACM385	KanR, pTGR5 derivative encoding P_{tac}_*riboE1-^{Cog}*lysZ* (gp25)	This paper
P_{tac}_*riboE_^{Cog}*lysZ*	pACM413	ApraR, pTGR5 derivative encoding P_{tac}_*riboE1-^{Cog}*lysZ* (gp25)	This paper
P_{tac}_*riboE_^{Corndog}*lysZ*	pACM583	ApraR, pTGR5 derivative encoding P_{tac}_*riboE1-^{Corndog}*lysZ* *(gp75)*	This paper
P_{tac}_*riboE_^{D29}*lysB*	pACM519	ApraR, pTGR5 derivative encoding P_{tac}_*riboE1-^{D29}*lysB* (*gp12*)	This paper
P_{tac}_*riboE_EV	pACM414	ApraR, pTGR5 derivative encoding P_{tac}_*riboE1 empty vector	This paper
P_{tac}_*riboE_^{Fury}*lysZ*	pACM489	ApraR, pTGR5 derivative encoding P_{tac}_*riboE1-^{Fury}*lysZ* (*gp59*)	This paper
P_{tac}_*riboE_*manC*	pACM488	ApraR, pTGR5 derivative encoding P_{tac}_*riboE1-*manC*	This paper
P_{tac}_*riboE_mptB	pACM514	ApraR, pTGR5 derivative encoding P_{tac}_*riboE1-*mptB*	This paper
P_{tac}_*riboE_*ppmC*	pACM491	ApraR, pTGR5 derivative encoding P_{tac}_*riboE1-*ppmC*	This paper
P_{tac}_*riboE_^{Smarties}*lysZ*	pACM594	ApraR, pTGR5 derivative encoding P_{tac}_*riboE1-^{Smarties}*lysZ* *(gp53)*	This paper
P_{tac}_CRISPR-array	pEWL003	CmR, pTGR5 derivative encoding P_{tac}-CRISPR array with BsaI digest sites for spacer editing	This paper
P_{tac}_EV	pACM352	KanR, pTGR5 derivative encoding P_{tac}_empty vector	This paper
P_{tac}_riboE-^{Cog}*lysZ*	pACM377	KanR, pTGR5 derivative encoding P_{tac}_riboE1-^{Cog}*lysZ*	This paper
P_{tac}_riboE-GFP	pACM040	KanR, pTGR5 derivative encoding P_{tac}_riboE1-GFP	This paper
P_{tac}-GFP	pACM246	CmR, pTGR5 derivative encoding P_{tac}-GFP	This paper
CL31 *ΔlysZ* editing plasmid	pACM321	CmR, pTGR5 derivative encoding CL31 editing template to delete *lysZ*	This paper
Cog *ΔlysZ* editing plasmid	pACM376	CmR, pTGR5 derivative encoding Cog editing template to delete *lysZ*	This paper

*A>G SNP between P_{tac} and riboE1.

Table S5. Primers used in this study.

Name	Sequence (5'-3')	Function	Ref.
ACM010	CATCTTGTTGTTACCTCCTTTAG	linearization of pEWL13	This paper
ACM103	TGTCCACATACAGACCAGAC	forward oligo to linearize pACM246	This paper
ACM125	CAATTCCACACATTATACGAGCCGATG	Reverse oligo to linearize pTGR5	This paper
ACM126	ATGGTGAGCAAGGGCGAGGAG	Forward oligo to linearize pTGR5	This paper
ACM128	CATCGGCTCGTATAATGTGTGGAATTGTGAGCGGAT AACAATTTGCTAGCGGTGATACCAGCATCGTCTTGAT GCCCTTGGCAGCACCCTGCTAAGGAGGTAACAACAA GATGGTGAGCAAGGGCGAGGAG	gBlock to insert riboE1 into pTGR5	This paper
ACM130	TGGTCCCACCTGACCCCATG	Forward oligo to linearize pTGR5	This paper
ACM133	CAAATTGTTATCCGCTCACAATTC	Reverse oligo to linearize pACM246	This paper
ACM140	CTACACACTCGGGCTGATAGC	Reverse oligo to screen and sequence Cog *ΔlysZ*	This paper
ACM155	CTTGTTGTTACCTCCTTAGCAGGG	Reverse oligo to linearize pTGR5 dativizes with riboE	This paper
ACM156	AGCGGCCGCTTAAGGTACC	Forward oligo to linearize pTGR5 derivatives	This paper
ACM159	CCCTGCTAAGGAGGTAACAACAAGATGCAGGCGCA CACTGTGCAG	Forward oligo to amplify CL31 *lysZ* with overhangs to pTGR5	This paper
ACM162	GGTACCTTAAGCGGCCGCTCTAATCATCATCGGGAT CATCGAGGG	Reverse oligo to amplify CL31 *lysZ* with overhangs to pTGR5	This paper
ACM354	GGTACCTTAAGCGGCCGCTCTTGTTGTTACCTCCTTA GCAGGG	Reverse oligo to create pACM414	This paper
ACM355	CCCTGCTAAGGAGGTAACAACAAGAGCGGCCGCTTA AGGTACC	Reverse oligo to create pACM414	This paper
ACM358	TTCGAATTTCTACTGTTGTAGATACCGCTGCAATAGC AAGAGGTGTCT	oligo to clone CL31 *lysZ* spacer into BseRI CRISPR array	This paper
ACM359	ACACCTCTTGCTATTGCAGCGGTATCTACAACAGTAG AAATTCGAAAC	oligo to clone CL31 *lysZ* spacer into BseRI CRISPR array	This paper
ACM366	CATATATGCGGCCGCATATTCAAACTTTGCTTGCTGT CCTGG	Upstream forward oligo to clone CL31 *ΔlysZ* editing template into pTGR5 derivatives	This paper
ACM367	GGGGGCAATACTAATCATCCGCCTGCATCACTCACC TGC	Upstream reverse oligo to clone CL31 *ΔlysZ* editing template into pTGR5 derivatives	This paper
ACM368	GCAGGTGAGTGATGCAGGCGGATGATTAGTATTGCC CCC	Downstream forward oligo to clone CL31 *ΔlysZ* editing template into pTGR5 derivatives	This paper
ACM369	GTGGTGGTGGTGAAGCTTAGGGCTGATGACATTGAT CTGC	Downstream reverse oligo to clone CL31 *ΔlysZ* editing template into pTGR5 derivatives	This paper
ACM370	CAAGCTCACTGCACTGCTCG	Forward oligo to detect and sequence CL31 *ΔlysZ*	This paper
ACM371	CCTGATGGACACACTCATGG	Reverse oligo to detect and sequence CL31 *ΔlysZ*	This paper
ACM372	GAATTGTGAGCGGATAACAATTTGCTAGCGTTTCTGA ATCTCCTCATCTAAGCAAGAGGAGTATCTCGTCTAGC GGCCGCTTAAGGTACCGAATTCTAAGCTTCACCACC ACCACCACCACTGACCTAGGTGCCTGGCGGCAGTA GCGCGGTGGTCCCACCTGACCCCATG	gBlock from IDT encoding Cas12 editable CRISPR array: BseRI cut sites, direct repeats, and overhangs with pACM246	This paper

ACM377	CTAAAGGAGGTAACAACAAGATGTCCATCTACCAAG AGTTTG	Forward oligo to clone ^{Fn}*cas12a* into pSEC01 from pJYS3	This paper
ACM378	CGACGGCCAGTGAATTCACGTGCTTAGTTATTGCGG TTCTGGAC	Reverse oligo to clone ^{Fn}*cas12a* into pSEC01 from pJYS3	This paper
ACM379	CTAAAGGAGGTAACAACAAGATGTCCATCTACCAAG AGTTTGTGAATAAATACTCCC	Upstream forward oligo to clone ^{Fn}*cas12a* D917A into pSEC01 from pJYS3	This paper
ACM380	GTTCGCCGCGAGCGATGGACAG	Upstream reverse oligo to clone ^{Fn}*cas12a* D917A into pSEC01 from pJYS3	This paper
ACM381	CTGTCCATCGCTCGCGGCGAAC	Downstream forward oligo to clone ^{Fn}*cas12a* D917A into pSEC01 from pJYS3	This paper
ACM382	CGGCCAGTGAATTCACGTGCTTAGTTATTGCGGTTC TGGACAAATTCAAAGTATTCTTCG	Downstream reverse oligo to clone ^{Fn}*cas12a* D917A into pSEC01 from pJYS3	This paper
ACM383	ATATCCCAACCTCTATCATC	oligo to sequence ^{Fn}*cas12a*	This paper
ACM384	TAACCCATCCAAGAAGGAAC	oligo to sequence ^{Fn}*cas12a*	This paper
ACM385	ATCAAGTTCTACAACCCATC	oligo to sequence ^{Fn}*cas12a*	This paper
ACM386	AACTACCACGACAAGCTGGC	oligo to sequence ^{Fn}*cas12a*	This paper
ACM391	GGAAGCAGCCCAGTAGTAGG	Forward oligo screen and sequence the inserts of pTGR5 derivatives	This paper
ACM392	GGCGTTTCACTTCTGAGTTC	Reverse oligo screen and sequence the inserts of pTGR5 derivatives	This paper
ACM399	GTCATCGTCGGGGTCATCGAGCTGCACTGTGTGCG CCTCCATC	Upstream reverse Cog *ΔlysZ* (gp26) editing template with ITA overhangs to pTGR5	This paper
ACM400	GATGGAGGCGCACACAGTGCAGCTCGATGACCCCG ACGATGAC	Downstream forward Cog *ΔlysZ* editing template with ITA overhangs to pTGR5	This paper
ACM402	ATTGGGGGAGAAGAGTGCTG	Forward oligo to screen and sequence Cog *ΔlysZ*	This paper
ACM403	CAGACTGTGCAGAGCACTGC	rev oligo to screen and sequence Cog *ΔlysZ*	This paper
ACM404	TTCGAATTTCTACTGTTGTAGATACCGCAGCAATAGC CAGAGGCGTCT	Forward oligo to clone Cog *lysZ* spacer into BseRI CRISPR array	This paper
ACM405	ACGCCTCTGGCTATTGCTGCGGTATCTACAACAGTA GAAATTCGAAAC	Reverse oligo to clone Cog *lysZ* spacer into BseRI CRISPR array	This paper
ACM421	TAGCGAAAGGATTTTTTACAGTGCTCGATCGCCTGAA GTCTC	Forward oligo to clone Fury *lysY-lysZ* into pTGR5	This paper
ACM422	GTGGTGGTGGTGAAGCTTAGTCAGACCCCGGCTCG CTTCC	Reverse oligo to clone Fury *lysY-lysZ* into pTGR5	This paper
ACM423	CATCGGCTCGTATAATGTGTGGAATTGTGAGCGGAT AACAATTTGCTAGCGAAAGGATTTTTTACACTAAGCT TCACCACCACCACCACCACTGACCTAGGTGCCTGGC GGCAGTAGCGCGGTGGTCCCACCTGACCCCATG	gBlock to make pTGR5-EV	This paper
ACM426	ATATATGCGGCCGCATATTCGCGCTGTCAAAACCTTT GCG	Upstream forward oligo to make Cog *ΔlysZ* editing template with ITA overhangs to pTGR5	This paper
ACM427	GTGGTGGTGGTGAAGCTTAGAAATCACCGCCTCCAC ATGG	Downstream reverse oligo to make Cog *ΔlysZ* editing template with ITA overhangs to pTGR5	This paper

ACM432	CCCTGCTAAGGAGGTAACAACAAGATGGAGGCGCACACAGTGCAG	Forward oligo to clone Cog *lysZ* into pACM40	This paper
ACM433	GGTACCTTAAGCGGCCGCTTTAGTCATCGTCGGGGTCATCG	Reverse oligo to clone Cog *lysZ* into pACM40	This paper
ACM434	GTGGTGGTGGTGAAGCTTAGTTATCCGTGGTCGGGAGTGG	Reverse oligo to clone Fury *lysY* into pACM414	This paper
ACM461	GGTACCTTAAGCGGCCGCTTCAGACCCCGGCTCGCTTCC	Reverse oligo to clone Fury gp58-59 into pACM414	This paper
ACM468	AGACAGGATGAGGATCGTTTCGCATGTCATCAGCGGTGGAGTGC	Forward oligo to amplify apmR cassette with tails for pTGR5 derivatives to get apramycin resistance	This paper
ACM469	CGAACCCCAGAGTCCCGCGCCAATCGACTGGCGAGCGG	Reverse oligo to amplify apmR cassette with tails for pTGR5 derivatives to get apramycin resistance	This paper
ACM476	CCCTGCTAAGGAGGTAACAACAAGATGGAAGTCCCACTCCCGAC	Forward oligo to amplify Fury *lysY* with overhang for pTGR5	This paper
ACM477	CCTGGTGTCCCTGTTGGATCGTTGTGATGGCAGACAATG	Upstream forward oligo for pCRD206 *Δcgp_0849* (*manC*)	This paper
ACM478	GGCTAAAAATGCCTACTGATCTAAAGTCATGTGTTCCTATTTCAC	Upstream reverse oligo for pCRD206 *Δcgp_0849* (*manC*)	This paper
ACM479	GTGAAATAGGAACACATGACTTTAGATCAGTAGGCATTTTTAGCC	Downstream forward oligo for pCRD206 *Δcgp_0849* (*manC*)	This paper
ACM480	GCATGCCTGCAGGTCGACTAACAATCGAGACCAAGAACG	Downstream reverse oligo for pCRD206 *Δcgp_0849* (*manC*)	This paper
ACM481	GCAAACTTAAACCACTATGC	sequencing oligo for *Δcgp_0849*	This paper
ACM482	TATCTGAATATTGATCCACG	sequencing oligo for *Δcgp_0849*	This paper
ACM548	GCTTGCGGATTCTGTCAACC	Upstream forward to clone *ΔmptA::kanR* for SOE recombineering template	This paper
ACM549	GAAAAATAAACAAATAGGGGTTCCGCGACGCGTCTACTACATCCGAC	Upstream reverse to clone *ΔmptA::kanR* for SOE recombineering template	This paper
ACM550	CATTTGATGCTCGATGAGTTTTTCTAATTGCATAAGGTAAACCGCCAC	Downstream forward to clone *ΔmptA::kanR* for SOE recombineering template	This paper
ACM551	GGTCAAGAAGGTGCTTTCATTCC	Downstream reverse to clone *ΔmptA::kanR* for SOE recombineering template	This paper
ACM552	ATGCGTACTGAGGTTATTGG	Forward oligo to detect and sequence *ΔmptA::kanR*	This paper
ACM553	GATACCTGTCCTCTAAAACG	Reverse oligo to detect and sequence *ΔmptA::kanR*	This paper
ACM554	GTCTAGGTGCCTGCGCACTC	Upstream forward to clone *ΔmptB::kanR* for SOE recombineering template	This paper
ACM555	GAAAAATAAACAAATAGGGGTTCCGCGAGTGTCGAGAAATTGGCGTAG	Upstream reverse to clone *ΔmptB::kanR* for SOE recombineering template	This paper
ACM556	CATTTGATGCTCGATGAGTTTTTCTAATTACACTGATCAACTGTGACTACTG	Downstream forward to clone *ΔmptB::kanR* for SOE recombineering template	This paper
ACM557	GAGGAAGATAATCTCAGGGCGACC	Downstream reverse to clone *ΔmptB::kanR* for SOE recombineering template	This paper
ACM558	TTTATCAGTAAGCCGATAAG	Forward oligo to detect and sequence *ΔmptB::kanR*	This paper

ACM559	AGCTCCCACACCATGTTGCG	Reverse oligo to detect and sequence *ΔmptB::kanR*	This paper
ACM560	GAACTTGGCTAAATTATGACGCG	Upstream forward to clone *ΔmptC::kanR* for SOE recombineering template	This paper
ACM561	GAAAAATAAACAAATAGGGGTTCCGCGGAAAAATAG TGTATCCGTATCCAG	Upstream reverse to clone *ΔmptC::kanR* for SOE recombineering template	This paper
ACM562	CATTTGATGCTCGATGAGTTTTTCTAAGCCTTACAGT CCGACAGCCTC	Downstream forward to clone *ΔmptC::kanR* for SOE recombineering template	This paper
ACM563	CCAGGCACGGTGTTGTCTTC	Downstream reverse to clone *ΔmptC::kanR* for SOE recombineering template	This paper
ACM564	AAGTTTTCTCCCAACCTATG	Forward oligo to detect and sequence *ΔmptC::kanR*	This paper
ACM565	ATGAGGTTGATGTTGTTGTC	Reverse oligo to detect and sequence *ΔmptC::kanR*	This paper
ACM581	CAATCGGTTCCGTGGGCAGTGTGCTTTGGTTTCACT AACCGGCAAGCAGTTTAGAAAAACTCATCGAGCATC AAATG	Forward oligo to recombineer Δ*ppmC::kanR* from pSEC01 template	This paper
ACM582	CGTCGAAAAGTAAAATAAAAACGTCCCGAAGGGACG AGGAGGACAACACCCGCGGAACCCCTATTTGTTTAT TTTTC	Reverse oligo to recombineer Δ*ppmC::kanR* from pSEC01 template	This paper
ACM583	GGCTGAAGAAGCAGAAAAGG	Forward oligo to detect and sequence Δ*ppmC::kanR*	This paper
ACM584	GGTGACAGTGTCCTTGAGTG	Reverse oligo to detect and sequence Δ*ppmC::kanR*	This paper
ACM585	AAGCTTATTTTGTTTAATTGAGTTTGAAGTTTTCCGTC GAAAGAGGCCATCGCGGAACCCCTATTTGTTTATTTT TC	Forward oligo to recombineer Δ*manA::kanR* from pSEC01 template	This paper
ACM586	AGATGTAGGCAAATCCTTGTTCTAATGCGGGCCTAG AGTTTGAACGAAGTTTAGAAAAACTCATCGAGCATCA AATG	Reverse oligo to recombineer Δ*manA::kanR* from pSEC01 template	This paper
ACM587	CTTTCAGGTAGATAATTCTG	Forward oligo to detect and sequence Δ*manA::kanR*	This paper
ACM588	GCTGAAGTAGATGTCAGTGG	Reverse oligo to detect and sequence Δ*manA::kanR*	This paper
ACM1166	TTAATTGAGTTTGAAGTTTTCCGTCGAAAGAGGCCAT TTGAGTTCCGAGTTCCGTGATGGTAACTTCACG	fwd oligo to clone *manA::kanR* lox from pEWL74 template	This paper
ACM1167	ATCCTTGTTCTAATGCGGGCCTAGAGTTTGAACGAA GTTTAGACAGGGTCAGCCGTCAATTGTCTGATTC	rev oligo to clone *manA::kanR* lox from pEWL74 template	This paper
ACM615	CCCTGCTAAGGAGGTAACAACAAGATGACTTTAACT GACAACAGC	Forward oligo to clone *manC* into pACM414	This paper
ACM616	GGTACCTTAAGCGGCCGCTCTACTGATCAGACGAAA AACG	Reverse oligo to clone *manC* into pACM414	This paper
ACM617	CCCTGCTAAGGAGGTAACAACAAGATGAGCAGTGAG GCAGTAGATG	Forward oligo to clone *ppmC* into pACM414	This paper
ACM618	GGTACCTTAAGCGGCCGCTTTAGAGCCAGGTGTTGC GCTTTTTG	Reverse oligo to clone *ppmC* into pACM414	This paper
ACM620	CCCTGCTAAGGAGGTAACAACAAGTTGCCGCGCATC GGCACCG	Forward oligo to clone *mptB* into pACM414	This paper
ACM621	GGTACCTTAAGCGGCCGCTTCAGTGTAAACCAAAGG TTGGATTCCGC	Reverse oligo to clone *mptB* into pACM414	This paper
ACM628	CCCTGCTAAGGAGGTAACAACAAGATGTCCAAGCCA TGGTTGTTTACCGTCCATGGTACCGGACAGCCAGAC CCACTCGGTCCTGGCCTGCCAGCGGATACTGCTCG CGATGTTCTTGACATTTATCGGTGGCAACCTATTGGT AACTATCCTGCCGCCGCGTTCCCAATGTGGCCATCC	gBlock to clone codon optimized D29 *gp12* (*lysB*) into pACM414	This paper

	GTAGAAAAGGGCGTAGCTGAGTTGATCTTGCAAATT GAATTGAAGTTGGATGCGGACCCGTATGCAGATTTC GCGATGGCAGGCTACAGCCAAGGTGCTATTGTAGTA GGTCAAGTGCTCAAACATCACATCCTGCCGCCTACG GGACGCTTGCATCGGTTCCTCCATCGGTTGAAAAAG GTCATCTTTTGGGGCAACCCAATGCGGCAGAAGGGT TTTGCCCACTCCGATGAATGGATCCACCCTGTCGCA GCCCCAGACACGCTGGGCATCTTGGAAGACCGCCT GGAAAACTTGGAGCAATATGGATTTGAGGTTCGGGA TTACGCTCATGATGGTGATATGTATGCATCTATCAAG GAGGATGACCTTCACGAATACGAAGTCGCGATTGGA CGTATCGTCATGAAGGCCTCTGGCTTCATCGGTGGA CGGGACTCTGTTGTCGCACAGTTGATTGAGCTGGGT CAACGTCCTATCACCGAGGGCATTGCCTTGGCAGGT GCGATTATTGATGCACTCACGTTTTTTGCGCGGTCAC GCATGGGTGATAAATGGCCCCATCTCTACAATCGGT ACCCAGCGGTAGAATTCCTGCGGCAGATTTGAAGCG GCCGCTTAAGGTACC		
ACM647	CCTGCTAAGGAGGTAACAACAAGTTGAGTTCCGAGT CCAGTCCTG	Forward oligo to clone *manA* into pAM414	This paper
ACM648	GGTACCTTAAGCGGCCGCTTTAGACAGGGTCCGTTT CCACG	Reverse oligo to clone *manA* into pAM414	This paper
ACM729	TAGCGAAAGGATTTTTTACAATGGTCCTGATCAGAAA GTTCGC	Forward oligo to clone Corndog *gp74-75* into pTGR5	This paper
ACM730	GTGGTGGTGGTGAAGCTTAGTCAACCACGGAGCATC TGGC	Reverse oligo to clone Corndog *gp75* into pTGR5	This paper
ACM731	CCCTGCTAAGGAGGTAACAACAAGATGAGCGTATTG GCCGAAGC	Forward oligo to clone Corndog *gp75* into pAM414	This paper
ACM732	GGTACCTTAAGCGGCCGCTTCAACCACGGAGCATCT GGC	Reverse oligo to clone Corndog *gp75* into pAM414	This paper
ACM751.2	GTGGTGGTGGTGAAGCTTAGTCATTCCCGTACGGCT CTCTC	Reverse oligo to clone pTGR5-Corndog *gp74* into pTGR5	This paper
ACM753	TAGCGAAAGGATTTTTTACAGTGATGTACAGCGGAC TGCCCACCGCCCAGCGGCGCGCGGTGAAGGCGTC GCTCATCGTCGGCTGGCTGTCCGCGACCGGCGCGG GACTCTCCGCGTGGTTGTTCCCGACGAGCGTGGTC CTGACGGGGATGGGCTACGCCGTCGCGGTCAGCAT GGGCATCACCCTGACCATTTCTGCCCTCCTCGCCGT GTACGGCGTGAGCGCGAACCGCTACCGGTTCGAGT GGGTGGCCGGGTGGCTCTCCGCGGCGTGCTTCGTG CCGTACAGCATCACCATCTGGTCCCTGACGATCACC GCCGAGTTGCACTGGCTGACAGCATCTTTCGTCTCG ACCGTCGCTCTGTCGTACTTCGTCTCCCGTGCCCTG CTCTGCGCCGCTCACGCGGCCAAGTTGCGGGTCGC CCACGAGACGAGTGACGCGATCACCTCTGCCATCG AGTCCGTACGAGAGGAGGGCGAGCATGGGGGAGAT GCTGGCCGTGCTAGCCGCCGAGACGAGTGACTAAG CTTCACCACCACCAC	gBlock of Smarties *lysY* with overhangs for pTGR5	This paper

ACM755	TAGCGAAAGGATTTTTTACAGTGATGTACAGCGGAC TGCCCACCGCCCAGCGGCGCGCGGTGAAGGCGTC GCTCATCGTCGGCTGGCTGTCCGCGACCGGCGCGG GACTCTCCGCGTGGTTGTTCCCGACGAGCGTGGTC CTGACGGGGATGGGCTACGCCGTCGCGGTCAGCAT GGGCATCACCCTGACCATTTCTGCCCTCCTCGCCGT GTACGGCGTGAGCGCGAACCGCTACCGGTTCGAGT GGGTGGCCGGGTGGCTCTCCGCGGCGTGCTTCGTG CCGTACAGCATCACCATCTGGTCCCTGACGATCACC GCCGAGTTGCACTGGCTGACAGCATCTTTCGTCTCG ACCGTCGCTCTGTCGTACTTCGTCTCCCGTGCCCTG CTCTGCGCCGCTCACGCGGCCAAGTTGCGGGTCGC CCACGAGACGAGTGACGCGATCACCTCTGCCATCG AGTCCGTACGAGAGGAGGGCGAGCATGGGGGAGAT GCTGGCCGTG	gBlock of Smarties *lysZ* with overhangs for *lysY* and pTGR5	This paper
ACM756	CCCTGCTAAGGAGGTAACAACAAGATGGGGGAGAT GCTGGCCGTGCTAGCCGCCGAGACGAGTGAGCCCT CGATGCCGTGGCTGACGCCACTCATCGCTCTCGGG ACTCTGCTCCTCGGATCGGGCGGCGTCGTCGCATG GCGGCGTCTGACTCACGACAAGCGGATCGGTGTCG CTCAGCAGGAGACGGCGGAGGACGACGCGCTGTCG AACCGGTGGCGGGCGATCATCGAGACGCAGACCAA AGTGCTCCTCGAACCCATGCAGGCGCAGATCGCGA CGCTGACGACCGAGGTGGCCGAGGTGAAAGTGGAA CTCGCCGAGTCCCGCCGTAAGTATTGGGGAGCCGT GGGGTACATCCGTACACTCCACAACTGGATCAACCG CCACCTGCCCGGCTCCGTCGAGCAGGTTCCCCCGC CTCCGGCGATCCTCGCCGAGGACATCTGAAGCGGC CGCTTAAGGTACC	gBlock of Smarties *lysZ* with overhangs for pAM414	This paper
ACM762	ATTGCAAGCGTTATTTTGTTCCCTAACCCCTTCGAGG ATTTATGCGTACCTCCGTGATGGTAACTTCACG	Forward oligo to recombineer *ΔpmmA::kanR lox* from pEWL74 template	This paper
ACM763	GGATAAGGAATTCCCGTGATGCCCGCCGGAAAATG GGATTATGCGCGGATAGCCGTCAATTGTCTGATTC	Reverse oligo to recombineer *ΔpmmA::kanR* lox from pEWL74 template	This paper
ACM880	TCGAAGGAAGAAGTCGATGC	Forward oligo to detect and sequence *Δcgp_0855::kanR lox*	This paper
ACM881	CAAAGTCGATGACGATGAGG	Forward oligo to detect and sequence *ΔpmmA::kanR lox*	This paper
ACM882	GACAATCAGCACGTCGAGCG	Reverse oligo to detect and sequence *ΔpmmA::kanR lox*	This paper
ACM990	TAGTCAAAGTCAAGGAAAGGACTTCAATCCCCGTGG TGCAAGTGGACAATTCCGTGATGGTAACTTCACG	Forward oligo to clone *Δcgp_0855::kanR lox* from pEWL74	This paper
ACM991	GTGCGCAGTGAGCCTTCCAATAGCTCCATTTACAAG TCCTTTTCTTCAATAGCCGTCAATTGTCTGATTC	Reverse oligo to clone *Δcgp_0855::kanR* lox from pEWL74	This paper

ACM992	GCGATGACTTCGTTGAGTGC	Reverse oligo to detect and sequence *Δcgp_0855::kanR lox*	This paper
AP195	CAAGAACACTGATCGCTGATCTCAAAGGCGAAGAATCACCATCGTCTCGCTCCGTGATGGTAACTTCACG	Forward oligo to recombineer *ΔmanA::kanR lox* from pEWL74 template	This paper
AP196	CTAAACCCTAGCGAGGAATACTTCTGCGTCCTCAGAACGCATCGCAATGGAGCCGTCAATTGTCTGATTC	Rev oligo to recombineer *ΔmanA::kanR lox* from pEWL74 template	This paper
AP239	CTGCGACGGACCTAGC	Forward oligo to detect and sequence *ΔmanA::kanR lox*	This paper
AP240	GAGCCAGACCAAACTAGGT	Reverse oligo to detect and sequence *ΔmanA::kanR lox*	This paper
AP001	TCCTGGTGTCCCTGTTGGATATTGAAAGAGGATAACGT	Upstream forward oligo for pCRD206 *Δcgp_1014* (*pmt*)	This paper
AP002	CCCTACCTTGGCGCTAACCTCCCCT	Upstream reverse oligo for pCRD206 *Δcgp_1014* (*pmt*)	This paper
AP003	TAGCGCCAAGGTAGGGCTTGGCTCACT	Downstream forward oligo for pCRD206 *Δcgp_1014* (*pmt*)	This paper
AP004	TGCATGCCTGCAGGTCGACTCTTCGATGACAACGGTG	Downstream reverse oligo for pCRD206 *Δcgp_1014* (*pmt*)	This paper
AP041	CCGAATACGAACTGTGG	sequencing oligo for *Δcgp_1014*	This paper
AP042	CCTGACCTGGTCTTTTACAT	sequencing oligo for *Δcgp_1014*	This paper
BH102	GCACGTGAATTCACTGGC	linearization of pSEC01 for creation of pEWL01 and pEWL102	(3)
BH103	CATCTTGTTGTTACCTCCTTTAG	linearization of pSEC01 for creation of pEWL01 and pEWL102	(3)
EWL035	TGCCTAATGAGTGAGCTAAC	linearization of pEWL3	This paper
EWL036	TCTCCTTACGCATCTGTGCGAAGCGCCTCATCAGCGGT	Amplification of P_{SOD}_riboE1:*dcas12* pEWL2	This paper
EWL037	GGCACCTAGGTTAGTTATTGCGGTTCTGGACAAATTCAAAG	Amplification of P_{SOD}_riboE1:*dcas12* pEWL2	This paper
EWL050	TTATTGCTCATTAGTTATTGCGGTTCTGGACAAATTCAAAG	*cas12a* from pEWL1 amplification	This paper
EWL051	CAATAACTAATGAGCAATAACTAGCATAAC	Terminator amplification T7 terminator from pTD68	This paper
EWL051	CAATAACTAATGAGCAATAACTAGCATAAC	Linearization of pEWL13 with overhangs for *cas12a* insertion via ITA	This paper
EWL052	GTTAGCTCACTCATTAGGCACTCCTTTCAGCAAAAAAC	Terminator amplification T7 terminator from pTD68	This paper
H019	ATCCAACAGGGACACCAGG	Forward oligo to linearize pCRD206 for isothermal assembly	
H020	AGTCGACCTGCAGGCATGC	Reverse oligo to linearize pCRD206 for isothermal assembly	
H021	CGCACAGATGCGTAAGGAG	linearization of pEWL3	This paper
J273	GCGGGACTCTGGGGTTCG	Reverse oligo to amplify pTGR5 and other plasmids to swap antibiotic cassette	This paper
J274	GCGAAACGATCCTCATCCTGTCT	Forward oligo to amplify pTGR5 and other plasmids to swap antibiotic cassette	This paper
J275	AGACAGGATGAGGATCGTTTCGCATGGAGAAAAAAATCACTGGATATACCACC	Forward oligo to amplify chlorR cassette from pFSC with overhangs to pTGR5 derivatives	This paper

J276	CGAACCCCAGAGTCCCGCTTACGCCCCGCCCTGCC	Reverse oligo to amplify chlorR cassette from pFSC with overhangs to pTGR5 derivatives	This paper
ATTB1g-UP	CTGAACATCATCGCAGTCATCCTCATTACG	Oligo to detect pK-PIM derivative plasmid integration site	(7)
ATTB1g-DN	CGGCGCACGGATCGAAGTGTTC	Oligo to detect pK-PIM derivative plasmid integration site	(7)
ATTB2g-UP	CATAAGTAGGGATAGTTGCCAAATCTGCTC	Oligo to detect pK-PIM derivative plasmid integration site	(7)
ATTB2g-DN	TGTCGAGAAACGAATGCCCCAGTTTCACCC	Oligo to detect pK-PIM derivative plasmid integration site	(7)

SUPPLEMENTAL MATERIALS AND METHODS

Plasmid Construction

pCRD206::*pmt* (pARP1)

PCR amplified pCRD206 backbone (AP53-54), 750bp upstream of *cgp_1014* and first 3 amino acids (AP1-2), and 750bp downstream including last 6aa of *cgp_1014* (AP3-4), assembled via ITA.

pCRD206::*ΔmanC* (pACM407)

PCR amplified pCRD206 backbone (H19/H20), ~1kb upstream and 3 amino acids (ACM477/478), and ~1kb downstream including last 2aa (ACM479/480), assembled via ITA.

P_{SOD}_*cas12* (pEWL001)

The vector pSEC1 was amplified using the primers BH102 and BH103. The Franciscella novicida *cas12* gene was amplified from pJYS3 using the primers ACM377 and ACM378 and assembled via ITA. pJYS3_ΔcrtYf was a gift from Sheng Yang (4) (Addgene plasmid # 85542 ; http://n2t.net/addgene:85542 ; RRID:Addgene_85542).

P_{SOD}_*cas12*_P_{tac}_anti-^{CL31}*lysZ*_spacer (pACM363)

Oligos ACM358/359 were annealed, PNK treated, and inserted into the pEWL018 CRISPR array via Golden Gate assembly using BseRI.

P_{SOD}_ *cas12*_P_{tac}_anti-^{Cog}*lysZ*_spacer (pACM351)

Oligos ACM404/405 were annealed, PNK treated, and inserted into the pEWL018 CRISPR array via Golden Gate assembly using BseRI.

P_{SOD}_ *cas12*_P_{tac}_CRISPR-array (pEWL018)

The vector pEWL3 was linearized with the primers EWL35 and H21. The catalytically inactive Francisella novicida *dcas12* under control of P_{SOD}-riboE1 was amplified from pEWL2 with the primers EWL36 and EWL37. The second insert contained a T7 terminator amplified from pTD68 with the primers EWL51 and EWL52. The vector and two inserts were assembled via ITA.

P_{SOD}_d *cas12*_P_{tac}_CRISPR-array (pEWL013)

The vector pACM246 was linearized with the following primers: ACM103 and ACM133. The CRISPR array containing the Type IIS restriction enzyme BseRI cut sites was ordered as a gBlock (ACM372) from IDT. The vector and gblock were ligated by ITA.

P_{tac}_*riboE_*manA* (pACM964)

PCR amplified pAM414 backbone (ACM155/156) and *manA* from MB001 gDNA (ACM647/648), assembled via ITA.

P_{tac}_*riboE_^{CL31}*lysZ* (pACM490)

PCR amplified pAM414 backbone (ACM155/156) and gp22 (*lysZ*) from CL31 gDNA (ACM159/162), assembled via ITA.

P_{tac}_*riboE_^{Cog}*lysZ* (pACM385)

pACM377 electroporated into MB001. Only got suppressors. Colony was picked and struck on BHI +/- IPTG theophylline to ensure that construct was still inducible. Sequencing revealed an A>G SNP between P_{tac} and riboE (*riboE).

P_{tac}_*riboE_^{Cog}*lysZ* (pACM413)

pACM385 linearized (J274/274) and apramacying resistance casette from pFSC (ACM468/469), assembled via ITA.

P_{tac}_*riboE_^{Corndog}*lysZ* (pACM583)

PCR amplified pAM414 backbone (ACM155/156) and *gp75* (*lysZ*) from Corndog gDNA (ACM731/732), assembled via ITA.

P_{tac}_*riboE_^{D29}*lysB* (pACM519)

PCR amplified pAM414 backbone (ACM155/156) and *lysB* from D29 codon optomized gBlock ACM628, assembled via ITA.

P_{tac}_*riboE_EV (pACM414)

pACM413 linearized (ACM354/355) with overlaps to create an empty vector, assembled via ITA.

P_{tac}_*riboE_^{Fury}*lysZ* (pACM489)

PCR amplified pAM414 backbone (ACM155/156) and *gp59* (*lysZ*) from Fury gDNA (ACM476/461), assembled via ITA.

P_{tac}_*riboE_*manC* (pACM488)

PCR amplified pAM414 backbone (ACM155/156) and *manC* from MB001 gDNA (ACM615/616), assembled via ITA.

P_{tac}_*riboE_*mptB* (pACM514)

PCR amplified pAM414 backbone (ACM155/156) and *mptB* from MB001 gDNA (ACM620/621), assembled via ITA.

P_{tac}_*riboE_*ppmC* (pACM491)

PCR amplified pAM414 backbone (ACM155/156) and *ppmC* from MB001 gDNA (ACM617/618), assembled via ITA.

P_{tac}_*riboE_^{Smarties}*lysZ* (pACM594)

PCR amplified pAM414 backbone (ACM155/156) and *gp53* (*lysZ*) from Smarties in gBlock ACM756, assembled via ITA.

P_{tac}_^{Corndog}*lysYZ* (pACM589)

pTGR5 digested with NdeI and EcoRI and *gp74-75* (lysY/*lysZ*) amplified from Corndog gDNA with ACM729/730, assembled via ITA.

P_{tac}_^{Corndog}*lysY* (pACM593)

pTGR5 digested with NdeI and EcoRI and *gp74* (lysY) amplified from Corndog gDNA with ACM729/751.2, assembled via ITA.

P_{tac}_CRISPR-array (pEWL003)

The vector pSEC1 was amplified using the primers BH102 and BH103. The Francisella novicida cas12 gene was amplified in two fragments from pJYS3 in order to introduce a D917A catalytic mutation. The first fragment utilized primers ACM379 and ACM380, while the second set of primers included ACM381 and ACM382. The vector and two inserts were assembled by ITA.

P_{tac}_EV (pACM352)

PCR amplified pTGR5 backbone (ACM125/130) and gBlock ACM423, assembled via ITA.

P_{tac}_^{Fury}*lysY* (pACM379)

pTGR5 digested with NdeI and EcoRI and *gp58* (*lysY*) amplified from Fury gDNA with ACM421/434, assembled via ITA.

P_{tac}_^{Fury}*lysYZ* (pACM349)

pTGR5 digested with NdeI and EcoRI and *gp58-59* (*lysY-lysZ*) amplified from Fury gDNA with ACM421/422, assembled via ITA.

P_{tac}_riboE-^{Cog}*lysZ* (pACM377)

PCR amplified pAM040 backbone (ACM155/156) and *lysZ* (gp26) from Cog gDNA (ACM432/433), assembled via ITA.

P_{tac}_riboE1-GFP (pACM040)

PCR amplified pTGR5 backbone (ACM125/126) and gBlock ACM128 with riboE1, assembled via ITA.

P_{tac}_^{Smarties}*lysY* (pACM592)

pTGR5 digested with NdeI and EcoRI and Smarties *gp52* (*lysY*) gBlock (ACM753) was assembled via ITA.

P_{tac}_^{Smarties}*lysYZ* (pACM595)

pTGR5 digested with NdeI and EcoRI and gBlocks (ACM755/756) encoding *gp52* and *gp53* (*lysY-lysZ*) were assembled via ITA

P_{tac}-GFP (pACM246)

PCR amplified pTGR5 backbone (J273/274) and chloroform resistance cassette (J275/276) from pFSC (5)

Δ^{CL31}*lysZ* editing plasmid (pACM321)

Digested pTGR5 with XbaI and EcoRI (removed P_{tac} and RBS), amplified ~200bp upstream and 3 amino acids (ACM366/367) and ~200bp downstream including last 2 amino acids (ACM368/369) of *gp22* (*lysZ*), assembled via ITA.

Δ^{Cog}*lysZ* editing plasmid (pACM376)

Digested pTGR5 with XbaI and EcoRI (removed P_{tac} and RBS), amplified ~200bp upstream and 6 amino acids (ACM426/399) and ~200bp downstream including last 7 amino acids (ACM400/427) of Cog *lysZ* (*gp25*), assembled via ITA.

References

1. Baumgart M, Unthan S, Rückert C, Sivalingam J, Grünberger A, Kalinowski J, et al. Construction of a Prophage-Free Variant of Corynebacterium glutamicum ATCC 13032 for Use as a Platform Strain for Basic Research and Industrial Biotechnology. Appl Environ Microbiol. 2013;79(19):6006–15.
2. McKitterick AC, Bernhardt TG. Phage resistance profiling identifies new genes required for biogenesis and modification of the corynebacterial cell envelope. Elife. 2022;11:e79981.
3. Hart EM, Lyerly E, Bernhardt TG. The conserved σD envelope stress response monitors multiple aspects of envelope integrity in corynebacteria. PLoS Genet. 2024;20(6 June).
4. Jiang Y, Qian F, Yang J, Liu Y, Dong F, Xu C, et al. CRISPR-Cpf1 assisted genome editing of Corynebacterium glutamicum. Nat Commun. 2017;8(May):1–11.
5. Peng F, Wang X, Sun Y, Dong G, Yang Y, Liu X, et al. Efficient gene editing in Corynebacterium glutamicum using the CRISPR/Cas9 system. Microb Cell Fact. 2017;16(1):1–13.
6. Ravasi P, Peiru S, Gramajo H, Menzella HG. Design and testing of a synthetic biology framework for genetic engineering of Corynebacterium glutamicum. Microb Cell Fact. 2012;11:147.
7. Oram M, Woolston JE, Jacobson AD, Holmes RK, Oram DM. Bacteriophage-based vectors for site-specific insertion of DNA in the chromosome of Corynebacteria. Gene. 2007;391:53–62.